Ore Geology Reviews 181 (2025) 106619

Contents lists available at ScienceDirect

Ore Geology Reviews

journal homepage: www.elsevier.com/locate/oregeorev

Constraining the fluid sources of gold-bearing veins in orogenic belts using sulfur and lead isotopes: A case study from Loch Tay, Scotland (UK)

Shane Webb [a,*], Taija Torvela [a], Rob Chapman [a], Lucia Savastano [a], Robert Jamieson [a], Adrian Boyce [b], Andrew Tait [b], Steven Hollis [c], Vanessa Pashley [d]

[a] Ores and Mineralization Group, University of Leeds, School of Earth and Environment, LS2 9JT, United Kingdom
[b] Scottish Universities Environmental Research Centre, Scottish Enterprise Technology Park, G75 0QF, United Kingdom
[c] School of Geosciences, Grant Institute, James Hutton Road, King's Buildings, Edinburgh EH9 3FE, United Kingdom
[d] British Geological Survey, Geochronology and Tracers, Keyworth NG12 5GG, United Kingdom

ARTICLE INFO

Keywords:
Gold
Exploration
Fluid mixing
$\delta^{34}S$
Pb isotopes

ABSTRACT

Unpicking the fluid and metal sources, and the number of mineralizing events, can be challenging because fluids from different origins mix and can overprint existing mineralization. Crustal and/or basinal fluids may play a role in "diluting" magmatic or mantle fluids and can have a significant impact on the isotope composition of the precipitated phases in an ore deposit, which ultimately leads to difficulties in classifying the deposit style. We present a case study of this problem from the southern margin of Loch Tay (Scotland). The results from sulfur and lead isotope studies indicate that magmatic-hydrothermal processes were responsible for the establishment of the mineralizing system, but this signature gets progressively obscured in some localities due to mixing between magmatic-hydrothermal and crustal fluids. Indications of two separate mineralization events have been observed, but differentiating the first stage from the second one is challenging. Our study demonstrates the need to understand the characteristics of the mineral system and the geological setting to support robust interpretation. The results also have implications for regional exploration models: we suggest that the majority of the auriferous vein occurrences at Loch Tay are probably of a magmatic origin, rather than of an "orogenic gold" type. Furthermore, the veins around Loch Tay provide a case study of how vein-hosted gold mineralization with some orogenic characteristics may be related to magmatism, suggesting that isotope data from other auriferous veins globally may be misinterpreted due to fluid mixing, particularly if the regional context is poorly understood.

1. Introduction

The formation of gold-bearing mineralization in orogenic terranes has been controversial (Goldfarb and Pitcairn, 2023), particularly regarding the origin of the mineralizing fluids. Previous researchers have suggested that meteoric (Pitcairn et al., 2006; Menzies et al., 2014), magmatic (Damdinov et al., 2021), metamorphic (Groves et al., 1998; Goldfarb et al., 2005; Phillips and Powell, 2010), and subcrustal fluids (Goldfarb et al., 2001; Goldfarb and Santosh, 2014; Groves et al., 2020) are involved in the mineralization processes, in varying proportions and depending on the deposit type in question (Goldfarb and Groves, 2015). Crucially, the vein-hosted gold deposit type referred to as "orogenic gold" is thought to form from mainly crustal fluid sources with no direct input from magmatic fluids (Ridley and Diamond, 2000; Yardley and Cleverley, 2013; Goldfarb and Groves, 2015; Goldfarb and Pitcairn, 2023) although, more recently, various authors have suggested an involvement of mantle-derived fluids (Groves et al., 2020). Significant overlaps between the 'magmatic' and orogenic' systems exist, however. Whilst magmatic gold-bearing mineralization is typically quite distinct in its mineralogy, mode of occurrence, and alteration (Sillitoe and Thompson, 1998; Thompson et al., 1999; Simmons et al., 2005; Sillitoe, 2010), some deposits in quartz ± carbonate veins resemble an orogenic deposit type ('gold only'; without extensive alteration) but show isotopic characteristics more compatible with a magmatic system, leading to a recognition that many magmatic gold deposits may have been misinterpreted as orogenic (Dirks et al., 2020; Lipson et al., 2024; McDivitt et al., 2021).

The situation is further complicated by the tendency for temporally

* Corresponding author.
E-mail address: SHWEB2@ulaval.ca (S. Webb).

https://doi.org/10.1016/j.oregeorev.2025.106619
Received 20 December 2024; Received in revised form 17 March 2025; Accepted 14 April 2025
Available online 16 April 2025

distinct episodes of mineralization (with potentially compositionally distinct fluids) to overprint one another; such relationships have been documented at several gold deposits globally (e.g., Fielding et al., 2018; Liu et al., 2020). Furthermore, mixing of hydrothermal and crustal fluids can have an impact on the isotopic signature of the precipitated phases, which poses challenges for interpreting fluid sources (Hill et al., 2013; Lambert-Smith et al., 2016). Potential strategies for reducing interpretational uncertainty include detailed paragenetic mapping (Webb et al., 2024a) and in-situ analyses, particularly when fluid mixing has occurred. Here, we use these strategies to investigate the isotope signature variability across multiple gold-vein occurrences near Loch Tay, Scotland. Our findings enable the assessment of the extent of both magmatic fluid flow and fluid dilution across the area, as well as the development of a new mineralization model for Loch Tay. Our study demonstrates approaches to address challenges in isotopic data interpretation and represents a contribution in the ongoing debate regarding why some auriferous quartz ± carbonate veins in orogenic belts may have been misinterpreted as orogenic.

2. Regional geology and metallogeny

The northern British Isles comprises several geological terranes (Fig. 1). The Grampian Terrane, which hosts our study area (Fig. 1), is mostly composed of a package of Neoproterozoic metasediments and volcaniclastics of the Dalradian Supergroup, deposited on the Laurentian margin (Stephenson et al., 2013). The composite Caledonian Orogeny (known as the Appalachian Orogeny in North America) resulted in a series of deformation episodes between the Ordovician and the Devonian, culminating in the closure of the Iapetus Ocean (McKerrow et al., 2000; Searle, 2021). The first deformation episode, the Grampian phase, occurred between c. 475–465 Ma and was characterized by a NW-SE collision between the Laurentian margin and various arc and microcontinental blocks of Avalonian affinity (Dewey, 2005; Cooper et al., 2011; Chew and Strachan, 2013; Tanner, 2014b; Rice et al., 2016; Molyneux et al., 2023). Peak metamorphism coincided with granitic magmatism following arc-ophiolite accretion and subduction reversal (Oliver, 2001; Baxter et al., 2002; Oliver et al., 2008; Cooper et al., 2011). Following the Grampian phase, a period of uplift occurred between c. 460–430 Ma (Soper et al., 1999; Moles et al. 2024). During this interval, the subduction of the Iapetus Ocean continued but magmatic events were less common, potentially due to a shallow angle of subduction and extensive erosion of the composite Laurentian margin (Miles et al., 2016; Moles et al., 2024).

The second stage of the Caledonian Orogeny, the Scandian phase, occurred between 435 and 410 Ma and is the most relevant for the present study (Dewey and Mange, 1999; Dallmeyer et al., 2001). During the Scandian, docking of Avalonia occurred against Laurentia in present-day Scotland and Ireland (Dewey and Strachan, 2003; Tanner, 2014a). Thrust tectonics were significant elsewhere but in the Grampian Terrane, no major crustal thickening or metamorphism occurred, the

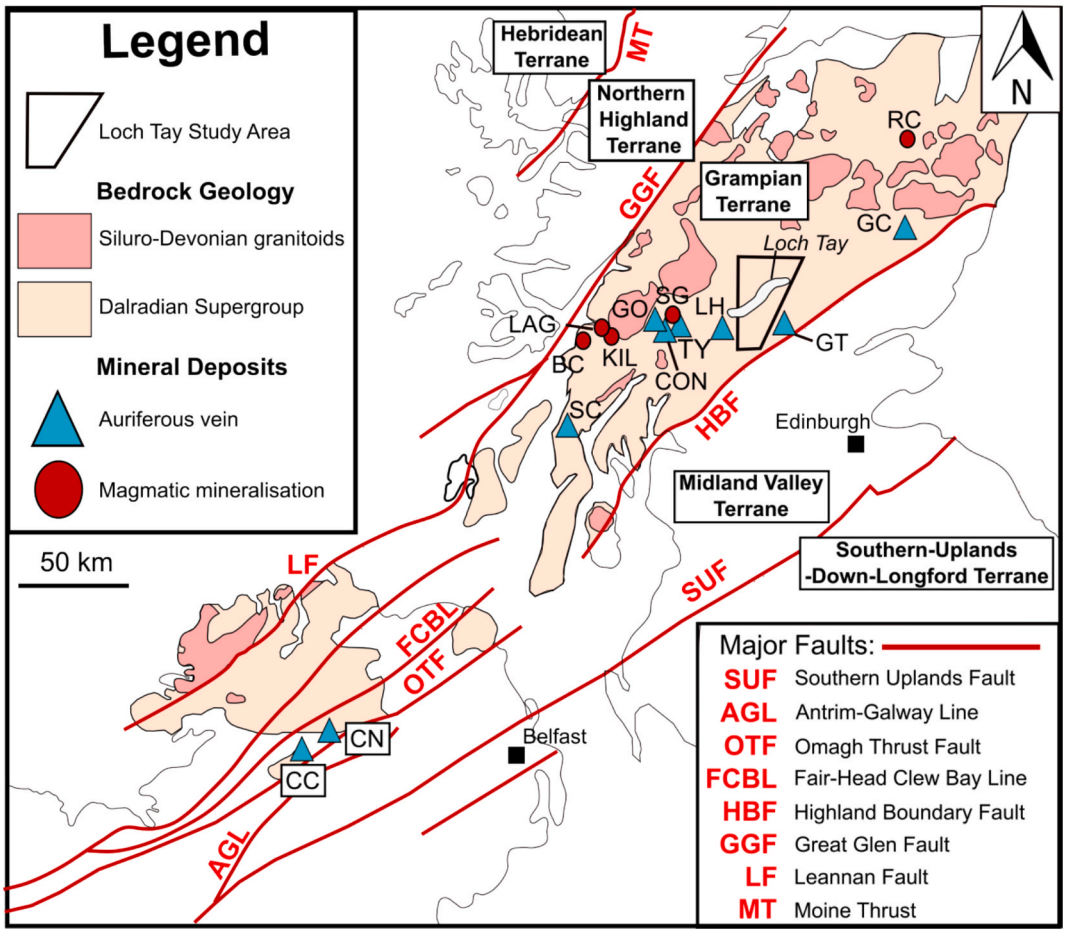

Fig. 1. Gold-bearing veins and magmatic gold mineralization in the Grampian Terrane (Shaw et al., 2022). The following abbreviations have been used: RC = Rhynie Chert (Baron et al., 2004), GC = Glen Clova (Smith et al., 2003), GT = Glen Turret (Smith et al., 2003), LH = Lochearnhead (Smith et al., 2003), TY = Tyndrum (Curtis et al., 1993), CON = Cononish (Rice et al., 2012), SG = Sron Garbh (Graham et al., 2017), GO = Glen Orchy (Hill et al., 2013), LAG = Lagalochan (Zhou, 1987), KIL = Kilmelford (Zhou, 1988), BC = Beinn nan Chaorach (Smith et al., 2003), SC = Stronchullin (Naden et al., 2010), CN = Curraghinalt (Rice et al., 2016), CC = Cavanacaw (Parnell et al., 2000). Furthermore, there are several occurrences of polymetallic mineralization around Loch Tay (Fig. 2), the outline of which is represented approximately using white infill.

deformation being mainly expressed by major sinistral strike-slip structures (Treagus, 2003; Tanner, 2014a). The transpression evolved into transtension around 425–410 Ma (Dewey and Strachan, 2003). This change coincides with the onset of widespread calc-alkaline igneous activity (the 'Newer Granites'; Oliver, 2001; Neilson et al., 2009). A genetic link between subduction and magmatism has been suggested (Thirlwall, 1982) although the lack of sedimentation post c. 420 Ma in the Southern-Uplands-Down-Longford Terrane accretionary prism implies that the subduction and closure of the Iapetus Ocean had ceased by this date. Late Caledonian magmatism persisted until 390 Ma, meaning that subduction alone cannot explain the occurrence of the magmatism (Oliver, 2001; Oliver et al., 2008; Miles et al., 2016). Alternative models involving post-collisional slab break-off/roll-back and asthenospheric upwelling have been suggested (Oliver et al., 2008; Neilson et al., 2009; Graham et al., 2017; Rice et al., 2018).

Regardless of the geodynamic drivers of magmatism, the NE-SW trending strike-slip/oblique-slip fault systems within the Grampian Terrane are likely to have facilitated the ascent of the plutons (Neilson et al., 2009; Rice et al., 2018). Tanner (2014a) considered the majority of the faults to represent Riedel shears that developed in response to shearing of the rock volume between the Great Glen Fault and Highland Boundary Fault. The larger faults in particular are very likely to be long-lived structures: for example, K-Ar dates from the Tyndrum Fault indicate this structure was still active at c. 410 Ma (Treagus et al., 1999). The final stage of the Caledonian-Appalachian Orogeny is known as the 'Acadian' phase, which is not well defined in Scotland. However, Acadian deformation, mostly in the form of strike-slip fault reactivation and minor folding, may have occurred from 400 to 390 Ma (Mendum and Noble, 2010; Chew and Strachan, 2013). The Acadian phase post-dates the mineralization concerned in our study (c. 425–417 Ma; Webb et al., 2024b) and is not discussed further.

In terms of metallogeny, the Grampian Terrane hosts many historical lead and copper mines (Wilson and Flett, 1921) but numerous auriferous vein systems also exist (Fig. 1). Few have drawn commercial interest: in Northern Ireland, gold has been extracted from Cavanacaw since 2005, whilst the development of Curraghinalt (one of the largest gold deposits in Europe) is ongoing (Dalradian Resources, 2018). Gold mining also occurred at Cononish between 2020 and 2023 (BBC News, 2023). In addition, several gold-bearing vein occurrences and prospects are known (e.g. in the Loch Tay area; Chapman et al., 2023). The gold is, in all cases, structurally controlled and related to Scandian transpressional-to-transtensional tectonics and strike-slip fault systems (e.g. Tanner, 2014a; Shaw et al., 2022). Although the structural association is clear, there are competing views regarding the type of gold mineralization and regional metallogeny in the Grampian Terrane. For example, Craw (1990), Craw and Chamberlain (1996), Pitcairn et al. (2015) and Parnell et al. (2017) propose an orogenic gold model for most known occurrences of gold mineralization in the region (e.g. based on fluid inclusion studies); regarding specific deposits, Rice et al. 2016 suggest that Curraghinalt is an orogenic gold deposit, given the high grade of the mineralization, the low salinity of fluids, the lack of alteration and the fact that there is no known coeval magmatism locally. Others consider a magmatic deposit model to be more likely; for example, Parnell et al. 2000 interpret the Curraghinalt fluid inclusion data to indicate a magmatic-hydrothermal system. At Cononish, Hill et al. (2013) and Spence-Jones et al. (2018) suggest a significant input from magmatic fluids with progressive mixing with sedimentary fluids, based on sulfur isotopes and Te signatures in the gold. Chapman et al. (2023), in turn, found both orogenic and magmatic signatures in a regional study of alluvial gold particles around Loch Tay. Therefore, more detailed investigation is required to better resolve the role of different fluids in the entire region. Only a single vein system is known at Cononish and Curraghinalt: consequently, to investigate the spatial changes associated with larger-scale mineralization, we turn our attention to Loch Tay where several mineralized vein systems resembling those at Cononish and Curraghinalt are known (Corkhill et al., 2010; Ixer et al., 1997).

2.1. Loch Tay geology and metallogeny

Before comparing isotope data from different localities and interpreting their regional significance, we first summarize the characteristics of the geology and mineralization in the Loch Tay area (Fig. 2; Fig. 3a-c). The region is dominated by the pelites and psammites of the Pitlochry Schist Formation, with some limestone and mafic to felsic metavolcanic intervals (Batchelor, 2004a, b; Stephenson et al., 2013). The majority of the mineralized veins in our study are hosted in metasiliclastics, with the exception of Coire Buidhe, which is hosted in limestone (Fig. 3c). It is also worth noting that the Foss and Duntanlich SEDEX deposits (Ba-Pb-Zn; Re-Os ages of c. 610 Ma; Moles and Selby, 2023) are situated just north of the study area (Fig. 1) and some authors suggest this horizon exists at depth in our study area due to overturned nappe tectonics (Treagus, 2000; Tanner, 2014a). Igneous bodies intrude the metasupracrustals within the Dalradian Supergroup. Six intrusions around Loch Tay have been dated (Fig. 2). The composite Comrie Pluton yielded ages of 425 ± 3 Ma (diorite) and 404 ± 6 Ma (granite; Oliver et al., 2008). Webb (2024) dated four felsic dykes throughout the region (Fig. 2); these ranged between c. 420–418 Ma.

The Loch Tay area hosts several gold and base metal occurrences (Figs. 2 and 3) and numerous alluvial gold particles have been retrieved in stream sediments throughout the region (Fig. 4). Several occurrences of the Loch Tay mineralization are close to the Loch Tay Fault (Fig. 2). Historic mining targeted mainly Coire Buidhe and the Finglen Vein (for lead and silver), and Tomnadashan (copper) (Pattrick, 1984; Ixer et al., 1997; Webb et al., 2024a,b). Both also contain some gold although it is volumetrically very minor (Pattrick, 1984; Webb et al., 2024b).

We distinguish between "magmatic mineralization" which has a clear link with porphyry intrusions (Tomnadashan and Comrie Pluton) and "vein systems" that outwardly resemble orogenic gold deposits (all the other occurrences). Collectively, and given the relative proximity of the know magmatic mineralization at Tomnadashan in particular, the vein-hosted mineralization around Loch Tay represents an ideal opportunity to investigate whether veins resembling 'orogenic' gold mineralization have in fact formed in response to magmatic processes. We describe the vein systems first. The auriferous veins in the Calliachar-Urlar area (Fig. 3a) and Tombuie (Fig. 3b) were discovered by Colby Gold in the 1980s. Further discoveries include discovery of gold mineralization by Erris Gold Resources at Lead Trial in 2019, and in the same year the authors discovered the auriferous vein at Glen Almond (Webb et al., 2024a, Fig. 2). None of these occurrences have to date been proven economic, but together they provide an ideal case study to investigate the characteristics of a regional metal-bearing hydrothermal event. Most of the veins around Loch Tay resemble orogenic gold veins rather than magmatic (porphyry-epithermal) mineralization: they have a relatively simple mineralogy (Table 1; Table 2), often massive textures, and in most cases lack intensive hydrothermal alteration or proven disseminated mineralization in the wallrock (Fig. 2).

Paragenetic interpretations have been published for the Glen Almond Vein (Webb et al., 2024a; Fig. 5) and broad mineralogical descriptions have been given by Ixer et al. (1997) for Calliachar-Urlar and Tombuie, and by Pattrick (1984), both complemented by the authors' own observations. Furthermore, Webb (2024) produced a preliminary paragenetic interpretation for Lead Trial (Fig. 5). The summary of the mineralogy of the vein systems is provided below and in Table 1.

Mineralogically, the auriferous veins have some broad similarities in that they all comprise quartz veins with galena, gold ± chalcopyrite, sphalerite and pyrite (Table 1). In most cases, the vein textures are massive with occasional vugs. Where detailed paragenetic interpretations are available, gold occurs typically in two paragenetic stages, with an earlier one usually as small inclusions within the pyrite and arsenopyrite (with very minor galena), and a later gold generation along fractures together with pyrite, sphalerite and chalcopyrite and, in places, silver tellurides (Ixer et al., 1997; Webb et al., 2024a,b). However, analysis of alluvial gold particles from the Calliachar-Urlar burns

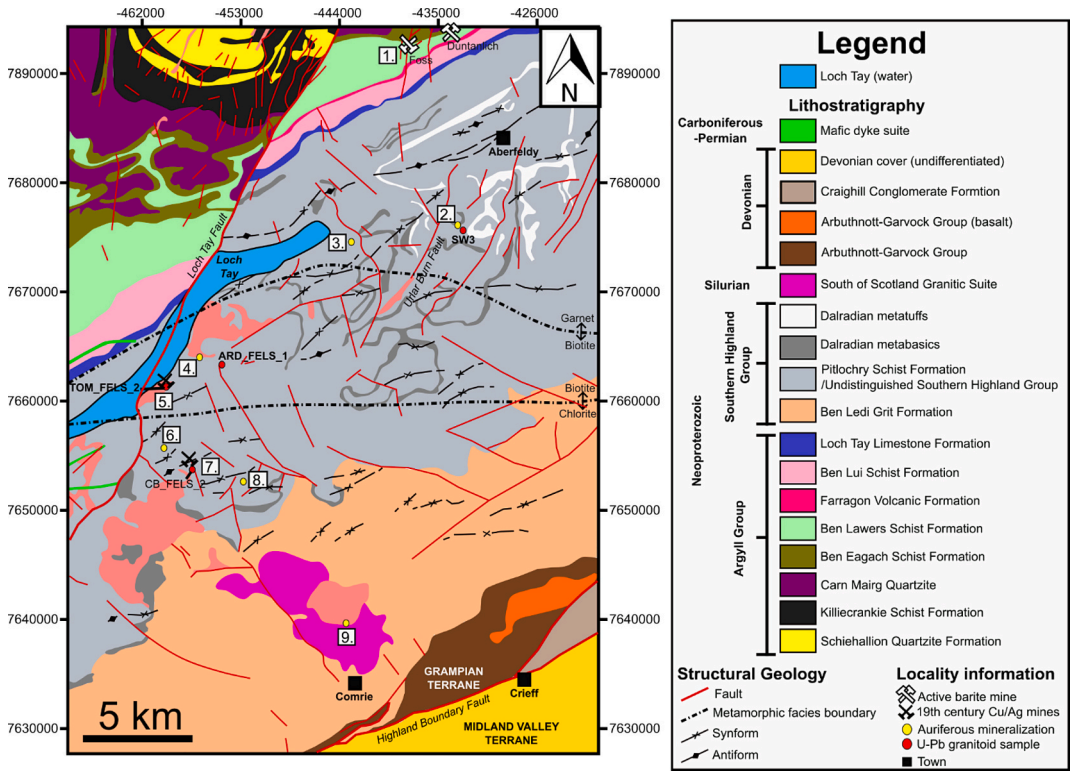

Fig. 2. Geological map of the Loch Tay study area, annotated with localities where polymetallic mineralization has been described. Numbers are as follows: 1 = Foss and Duntanlich (Foss closed in 2021 and is represented by downward facing arrows, whilst operations at Duntanlich are ongoing), 2 = Calliachar and Urlar, 3 = Tombuie, 4 = Lead Trial, 5 = Tomnadashan, 6 = Finglen Vein, 7 = Coire Buidhe, 8 = Glen Almond Vein, 9 = Comrie Pluton. Several sources were used to compile the geological information (Bradbury and Smith, 1981; Searle, 2021; Digimap, 2023). The terms 'TOM_FELS_2', 'ARD_FELS_1', 'CB_FELS_2', and 'SW3' represent granitic dykes that were dated to c. 420–418 Ma via CA-ID-TIMS U-Pb geochronology (Webb, 2024).

and Glen Almond (Fig. 4) has revealed a more complex mineralogy not necessarily captured by the in-situ samples (e.g. the presence of tellurides, pyrrhotite, arsenopyrite, gersdorffite cobaltite, sulfosalts as inclusions within the gold; Ixer et al. 1997; Chapman et al., 2023). A late galena ± sphalerite-bearing stage is also identified (without gold).

Lead Trial and Coire Buidhe are slightly different to the other veins systems: the vein textures resemble those reported from low sulfidation epithermal mineralization globally (vuggy quartz, extensive brecciation, sheeted quartz indicative of several episodes of fracturing; Cooke and Simmons, 2000), although it should be noted that textural features within a hydrothermal vein do not necessarily serve as a reliable indication of deposit type. Lead Trial also contains very little pyrite, whereas in the other veins pyrite is common. Furthermore, at Coire Buidhe, Pattrick (1984) reported the presence of Pb-Bi-Ag sulfosalts and native bismuth, which is not typical of the other gold-bearing vein systems (Table 1).

The 'magmatic' mineralization at Tomnadashan and the Comrie Pluton, in contrast, is quite distinct from the vein systems. Two paragenetic stages have been identified at Tomnadashan; a disseminated assemblage within the host rocks, mainly comprised of molybdenite, tetrahedrite, pyrite and chalcopyrite; and a later, quartz ± carbonate vein-hosted mineralization with copper sulfosalts, galena, native bismuth and other Bi-phases, and sphalerite (Pattrick, 1984; Webb et al., 2024b). The Comrie Pluton aureole is seen to contain disseminated arsenopyrite, chalcopyrite, molybdenite and pyrite (Naden et al., 2010; Webb, 2024).

2.2. Existing genetic models

There is evidence in support of the classification of Tomnadashan as a Cu-Mo porphyry deposit. The mineralogy of Tomnadashan (Pattrick, 1984; Webb et al., 2024b) is very similar to that which has been reported from porphyry deposits globally (Sillitoe, 2010). Additionally, the limited published $\delta^{34}S$ data (between 0 and +2 ‰; Lowry et al., 2005) are consistent with a magmatic-hydrothermal fluid source, and the age of mineralization (c. 417–425 Ma; molybdenite Re-Os, Webb et al., 2024b) closely overlaps with ages derived from granitic dykes both at Tomnadashan and throughout the wider Loch Tay region (c. 420–418 Ma; Webb, 2024). The distribution of alteration haloes is consistent with genetic models for porphyry mineralization (Sillitoe, 2010), with potassic alteration associated with the granitic dykes injected into the country rock (Webb et al., 2024b). For the Comrie Pluton, a disseminated assemblage dominated by pyrite, arsenopyrite and chalcopyrite is associated with the potassic alteration confined to the granitic portion of the pluton (Fig. 2; Naden et al., 2010).

The regional mineral system and the deposit model for the gold-bearing veins is, by contrast, much less clear and the general assumption has been that they represent a system that is different to the magmatic mineralization (Pattrick, 1984; Corkhill et al., 2010; Webb et al., 2024b). Signatures compatible with both a magmatic system and orogenic gold have been observed, but the work to date has been inconclusive. A magmatic origin has been proposed for Coire Buidhe, largely based on the mineralogy (Pattrick, 1984; Corkhill et al., 2010; Naden et al., 2010; Smith et al., 2022), although Pattrick (1984) suggested that the geographically restricted alteration haloes of Tomnadashan and Coire Buidhe meant that the two were unlikely to comprise the same magmatic-hydrothermal system. Corkhill et al. (2010) used stream sediment data collected in the wider region by the British Geological Survey (Johnson and Breward, 2004) and noted that several of the mineralized localities around Loch Tay (Tombuie, Coire Buidhe and Calliachar-Urlar) displayed elevated bismuth concentrations, which were tentatively considered to be comparable with magmatic-hydrothermal systems globally. Chapman et al. (2023) studied the microchemical characteristics of alluvial gold particles collected from

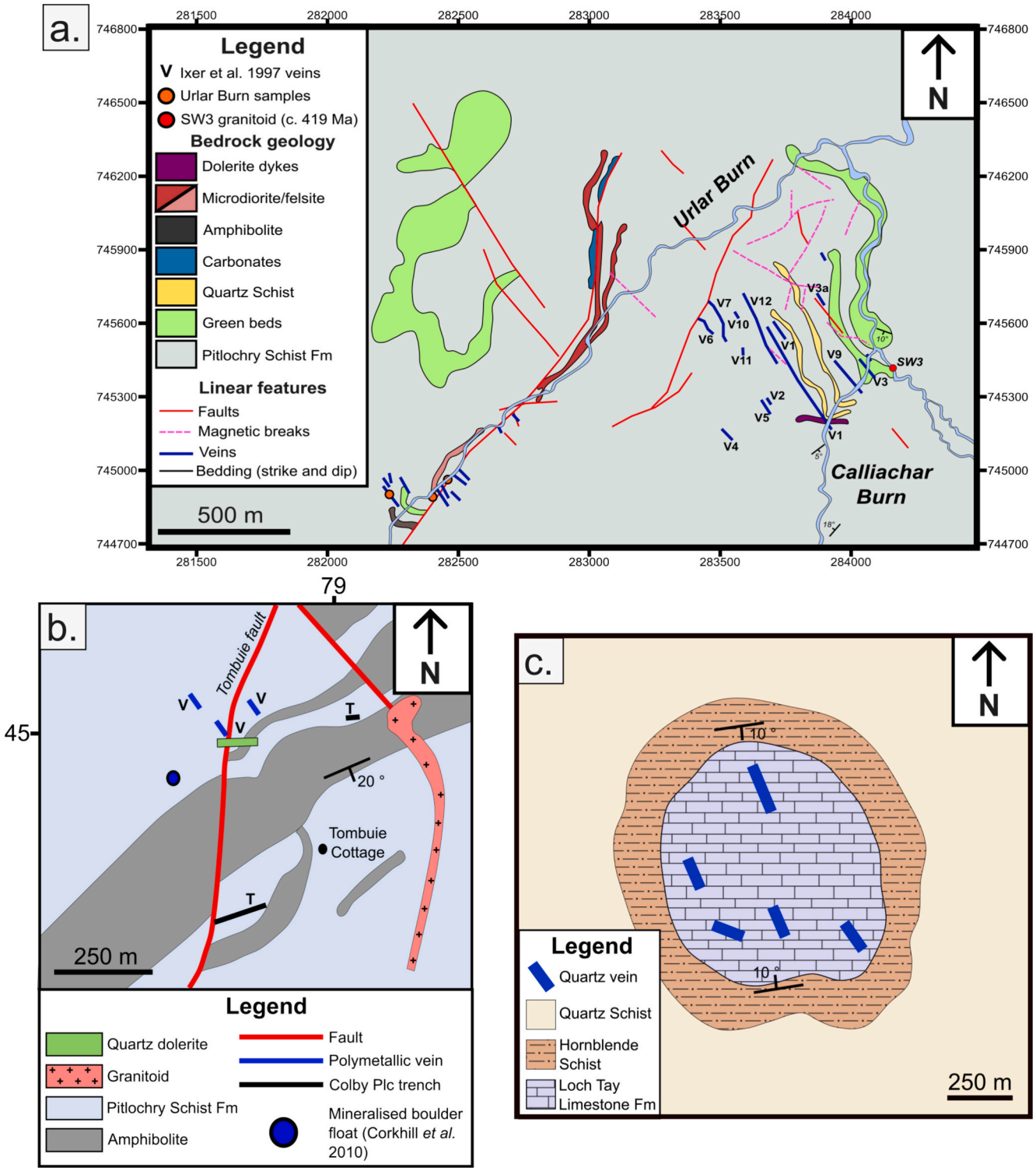

Fig. 3. Geological maps of individual prospects of interest. a. The different veins, each identifiable by a distinct 'V' number (Ixer et al., 1997), in the Calliachar and Urlar burns (collectively referred to as'CUB'). The strike and dip measurements of the bedding were collected by Webb (2024). b. Tombuie (Corkhill et al., 2010). c. Coire Buidhe (Pattrick, 1984). In this region, the limestone represents a small, isolated lenses overlying the rest of the Dalradian metasedimentary package.

across the Loch Tay area (Fig. 4): they reported two categories of gold particles, orogenic and porphyry/epithermal, based on the similarities of the microchemical signatures to other regions with established genetic models. This was the first finding indicating that a variety of fluid sources may have been involved in the development of gold mineralization around Loch Tay.

Previous isotope data from the region around Loch Tay are limited to a few $\delta^{34}S$ values derived by Smith (1996) and Lowry et al. (2005) from Calliachar-Urlar, Coire Buidhe, Tombuie, Tomnadashan and the Comrie Pluton (Fig. 6). The data mostly cluster outside of the various ranges suggested typical for magmatic sulfur (i.e. $< +5$ ‰; Ohmoto, 1972; 1986; Labidi et al., 2013; Hutchison et al., 2020). However, no paragenetic or mineralogical context were provided for the data by either author. Fluid inclusion data from the different localities within the study

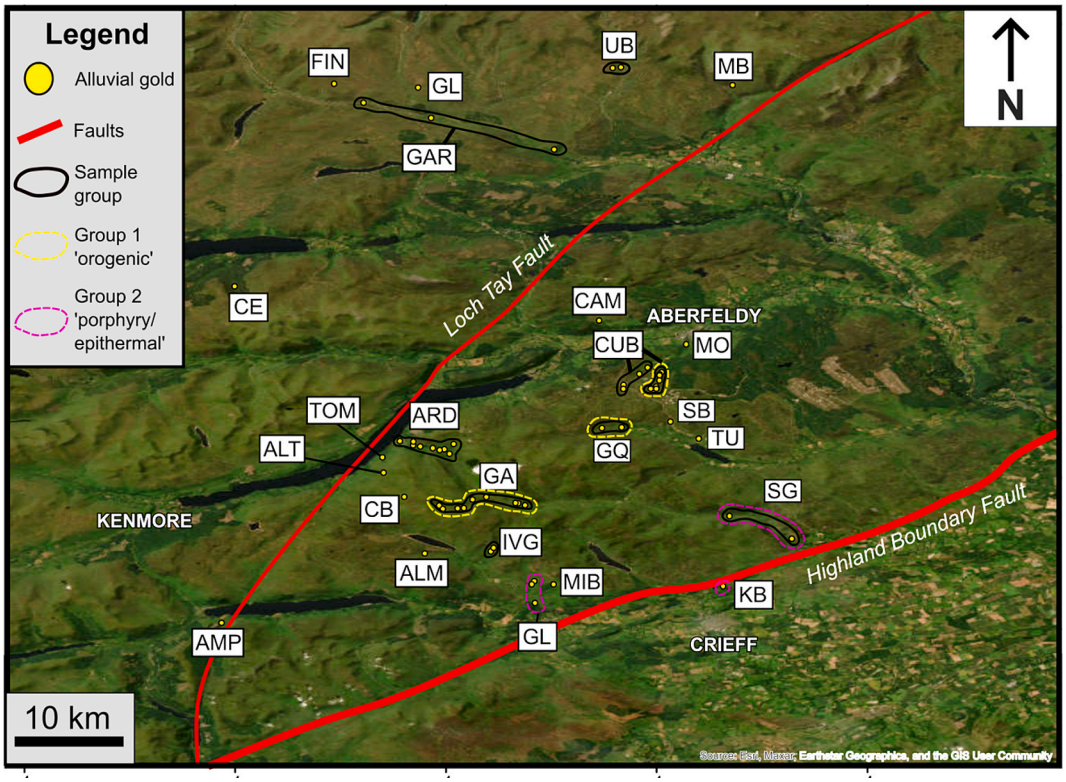

Fig. 4. Satellite image of the Loch Tay region depicting localities where alluvial or detrital gold has been retrieved. The'Group 1′ and'Group 2′ populations are categories recognized by Chapman et al. (2023). The following abbreviations have been used: ALM = Alt Mathaig, ALT = Allt A Mheinn, AMP = Ample, ARD = Ardtalnaig Burn, CAM = Camsernay, CB = Coire Buidhe (detrital gold from spoil heaps), CE = Carrie, CUB = Calliachar-Urlar Burns, FIN = Finglen (not to be confused with the Finglen Vein, this distinct geographical feature shares a similar name), GAR = Garry, GA = Glen Almond, GAR = Garry, GL = Glen Lyon, GQ = Glen Quaich, IVG = Invergeldie, KB = Keltie Burn, MB = Monzie, MIB = Milton Burn, MO = Moness, TOM = Tomnadashan, TU = Tuerrich, SB = Shian Burn, SG = Sma Glen. Here, the term 'sample group' is intended to denote a group of samples that have been collected from the same stream. The locations have been compiled from many previous publications (Chapman et al., 2000, 2002, 2023), although several localities where gold has been panned by researchers from the University of Leeds have not been reported anywhere (ALM, ALT, CAM, IVG, MO, CE, and ARD).

Table 1
Mineralogy of the known in-situ localities around Loch Tay. At all localities, quartz ± carbonate veins have been recorded. Only the most abundant ore minerals have been described, demonstrating the broad similarities and localized differences between the different localities, based on our own observations and those from several previous studies (Pattrick, 1984; Ixer et al., 1997; Corkhill et al., 2010; Naden et al., 2010; Smith et al., 2022; Webb et al., 2024a,b). The 'Abbreviation' column indicates the abbreviations used for each locality in Fig. 3, Fig. 4, Fig. 8, and Fig. 9.

Name	Abbreviation	Bismuth phases	Tetra-hedrite	Arseno-pyrite	Chalco-pyrite	Galena	Molyb-denite	Pyrite	Pyrrhotite	Sphale-rite	Nickel sulfides	Cobaltite
Gold-bearing vein systems												
Tombuie	TB			✓	✓	✓		✓	✓	✓	✓	✓
Calliachar-Urlar	CUB			✓	✓	✓		✓	✓	✓	✓	✓
Lead Trial	LDT				✓	✓				✓		
Finglen Vein	FV			✓	✓	✓		✓	✓	✓	✓	
Coire Buidhe	CB	✓			✓	✓		✓		✓		
Glen Almond Vein	GAV				✓	✓		✓		✓		
Magmatic systems												
Tomnadashan	TOM	✓	✓		✓	✓	✓	✓		✓		
Comrie Pluton	CP			✓	✓		✓	✓				

area is compiled in Table 3, although these previous studies lack paragenetic context. For example, it is unknown whether the hotter, Type 1 inclusions (350 °C) precede or postdate the Type 4 inclusions (91–175 °C) in the Calliachar-Urlar burns (Table 3). Nonetheless, the localities show a very broad range in the homogenization temperature. Ixer et al. (1997) interpreted the range in fluid inclusion temperatures recorded from Calliachar-Urlar to reflect a hotter, deeper fluid mixing with meteoric fluids, and suggested that the Urlar Burn Fault (Fig. 3a) was the main conduit facilitating transportation of the deeper fluid. Ixer et al. (1997) further suggested that the gradual variations in gold composition indicate that the Calliachar-Urlar veins comprise a single mineralizing system (as opposed to temporally separated fluid pulses). Corkhill et al. (2010) considered the veins at Tombuie (Fig. 3b) to share a genetic link to the Calliachar-Urlar mineralization based on the similarities in mineralogy, strike of the veins and the occurrence of mercurian electrum. None of the previous studies have, however, made a wider assessment of the genetic relationships of the various mineralized occurrences around Loch Tay.

Table 2
Compilation of the different categories of veins in the Calliachar and Urlar burns, as described by Ixer et al. (1997).

Vein Type	Description
High grade gold	Veins 1, 3, 6 and 7. Contain galena, pyrite, sphalerite, chalcopyrite, arsenopyrite, and electrum. Wallrock alteration (described as 'bleaching') occurs up to 20 m away from the contact margins of these veins. Gold grades of 77–150 and 480 g/t were reported from V6 and the gossan, respectively.
Base metal	Veins 2, 4, 5, 8 and 12; Contain galena, chalcopyrite, sphalerite, pyrite and arsenopyrite. Wallrock alteration is minimal. Gold grades were reported for V5 (0.5 g/t) and V12 (<2 g/t).
Barren	Quartz veins with no notable sulfide mineralization.

3. Samples and methods

In total, 73 rock samples were collected. These were analysed for their $\delta^{34}S$ signatures (both in-situ and bulk) and Pb isotope ratios (from galena) as detailed below. To facilitate accurate interpretation of isotope data, paragenetic analyses from previously published studies by the authors were used to contextualize the analysed material (Fig. 5; Webb et al., 2024a, b; Webb, 2024). It should be noted that tabulated results for the sulfur and lead isotope analyses can be found in Supplementary Material A and B (Table A1; Table A2; Table B1); furthermore, co-ordinates for each sample are provided in Supplementary Material C (Table C1).

3.1. $\delta^{34}S$ analyses

The $\delta^{34}S$ signatures were determined for pyrite, chalcopyrite, galena, molybdenite and/or arsenopyrite, depending on the mineralogy at each locality and which phases were available in sufficient quantities for analysis. Both bulk and in-situ analyses were used, conducted at the University of Leeds and the Scottish Universities Environmental Research Centre (SUERC) at the University of Glasgow. The in-situ $\delta^{34}S$ data have the specific advantage of enabling the data to be linked to the paragenetic context. The bulk $\delta^{34}S$ data have a better efficiency-cost ratio, although the paragenetic context of each measurement is lost and the analysed sample can contain material from more than one paragenetic stage. It should also be noted that the results of previous sulfur isotope studies in Scotland and Ireland are presented in Fig. 6.

3.1.1. Bulk $\delta^{34}S$ analyses

93 analyses from 73 samples representing 9 localities (Fig. 2) were conducted in the Cohen Geochemistry Laboratory at the University of Leeds. The analyses utilized an Elementar PYRO cube coupled to an IsoPrime continuous flow mass spectrometer in accordance with the methodology described in He et al. (2020). Sulfide powders were obtained by Dremel drilling sulfide grains separated from a crushed rock sample. The powders were placed into tin cups prior to ignition at temperatures of approximately 1150 °C; a flow of both helium and pure oxygen of the CP and N5.0 grades respectively was used (He et al., 2020). The gas was funnelled through tungsten oxide; excess oxygen was removed from the gas stream using pure copper wires held at 850 °C, and water was removed using SICAPENT. The SO_2 was separated from N_2/CO_2 by temperature-controlled adsorption/desorption columns. To calculate the $\delta^{34}S$ of each sample, the cumulative mass spectral signals at m/z 64 and 66 from the sample were normalized to those of an SO_2 reference gas (N3.0). These values were calibrated to the international V-CDT scale using a seawater-derived lab barium sulphate standard, SWS-3, which has been analyzed against the international standards NBS-127 (20.3 ‰), NBS-123 (17.01 ‰), IAEA S-1 (−0.30 ‰), and IAEA S-3 (−32.06 ‰) and assigned a value of 20.3 ‰, and an interlab chalcopyrite standard CP-1 assigned a value of − 4.56 ‰. The precision obtained for repeat analysis of a laboratory check standard $BaSO_4$ is ±0.3 ‰ (1 SD) or better

3.1.2. In-situ $\delta^{34}S$ analyses

54 measurements from 11 polished blocks representing 6 localities were derived via in-situ $\delta^{34}S$ analyses using a laser ablation inductively-coupled plasma mass spectrometer at SUERC. The method was originally developed by Kelley and Fallick (1990); the laser sulfur system was developed in-house and consists of three key systems: The laser system (i.e. The laser, microscope, motorized X-Y-Z stage, imaging system and the vacuum chamber), a vacuum line to purify the gas, and a mass spectrometer to perform the measurement. The laser is a CGI Laser FL-1064-CW 30-Watt diode with pumped neodymium-doped yttrium aluminium garnet (Nd: YAG), which provided a 1064 nm beam focused to a spot size of ~ 80 μm. The laser was fired across a 0.25 mm^2 portion of the sample to combust the sulfide and produce SO_2 which is transferred to the mass spectrometer (a VG Isotech Optima with a Nier type gas source, a small radius analyzer and three fixed Faraday cups) configured to measure masses 64 and 66 along with a reference gas of known composition. Individual measurements of an internal chalcopyrite (CP1) standard were used alongside those of the NBS 123 (sphalerite) and IAEA-S-3 (silver sulfide) standards, to plot a 3-point regression line, from which the sample $\delta^{34}S$ data could be calibrated. SO_2 (g) for these standards and individual mineral samples, drilled out of a polished block, were generated on the conventional vacuum extraction line for S. The average difference of repeat measurements (at least triplicate) of each mineral between the conventional and laser-ablation systems was used to correct the final $\delta^{34}S$ values. The $\delta^{34}S$ data were corrected following the procedure of Kelley and Fallick (1990), with the resulting precision of the analyses being consistently better than ±0.3 ‰. The small isotopic fractionation associated with the laser combustion of sulfide minerals is taken into account in the calculations.

3.2. Pb isotopes

42 measurements from 33 samples representing 9 localities were obtained. A Dremel drill was used to extract galena powder from hand specimens; the powders were dispatched to the geochronology and Tracers Facility at the British geological Survey and the National Centre for isotope Geochemistry, University College Dublin (UCD).

For the Pb isotope analyses, 1 ml 2 M Teflon distilled HNO_3 was inserted into each vial, after which each sample was dissolved through heating to temperatures of > 100 °C over 24 h. A Thermo Fisher Scientific Neptune Plus MC-ICP-MS instrument, coupled with a Jet Interface, was used to measure the Pb isotope ratios. Prior to analysis, samples were diluted with 2 % Teflon-distilled nitric acid and spiked with a thallium solution at a ratio of approximately 1 thallium to 10 lead. The isotopes measured simultaneously included ^{202}Hg, ^{203}Tl, $^{204}Pb/Hg$, ^{205}Tl, ^{206}Pb, ^{207}Pb, and ^{208}Pb. Each acquisition involved 75 ratio measurements, each with a 4.2-second integration time. Baseline measurements were defocused for 60 s before each acquisition. The precision of the method was assessed by repeatedly analyzing the NBS 981 Pb reference solution, which was also spiked with thallium. The computed average values for the NBS 981 isotopic ratios were then juxtaposed with the known isotopic ratios for this reference material (Thirwall, 2002). The sample data were normalized using the average relative deviation of measured reference values from their true counterparts. Internal uncertainties, stemming from the reproducibility of measured ratios, were propagated relative to external uncertainties, such as those associated with the reproducibility of NBS 981 reference material.

4. Results

4.1. $\delta^{34}S$ data

$\delta^{34}S$ results from this study are compiled in Supplementary Material A (Table A1; Table A2). In the Loch Tay region, the $\delta^{34}S$ values range from –2 to +13 ‰ (Figs. 7, 8). Around Tomnadashan and Lead Trial, the

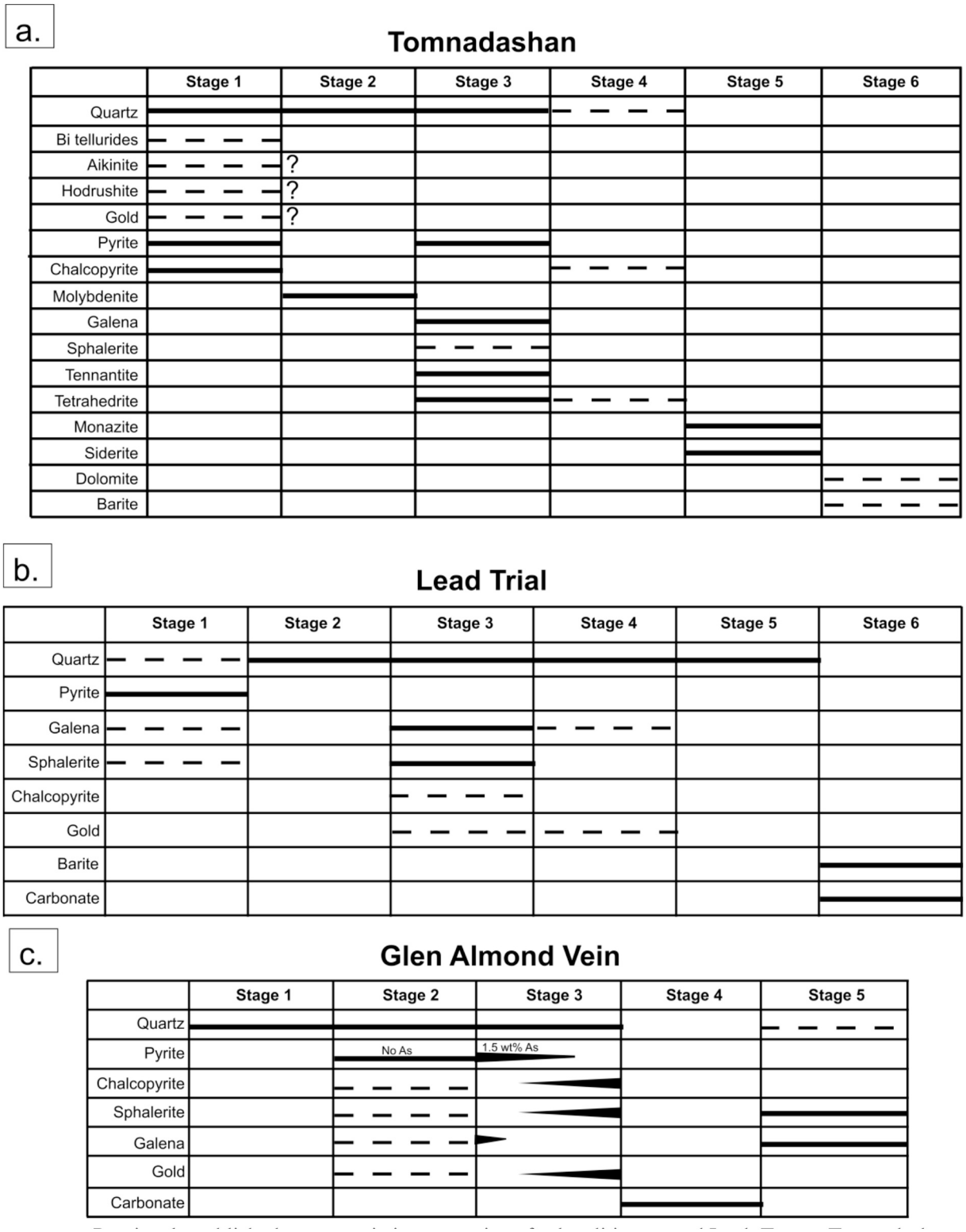

Fig. 5. Previously published paragenetic interpretations for localities around Loch Tay. a. Tomnadashan (Webb et al., 2024b). The question marks indicate phases that were described and interpreted by Pattrick (1984) but not observed in the more recent studies of vein parageneses. Regarding gold, Webb et al., 2024b suggested that the discovery of bismuth tellurides within gold particles retrieved from Tomnadashan was evidence that gold occurs within the first paragenetic stage. b. Lead Trial (Webb, 2024). c. The Glen Almond Vein (Webb et al., 2024a).

$\delta^{34}S$ signatures are typically between 0 and +5 ‰ whilst the veins in the eastern part of the study area (Tombuie, Calliachar-Urlar) on one hand, and in Finglen Vein on the other hand, yield isotopically higher values of +6 to +13 ‰ (Fig. 7a-c; Fig. 8). We interpret these differences in the light of typical 'magmatic' and 'crustal' sulfur isotope profiles as discussed by Hutchison et al. (2020): for example, typical 'magmatic' (porphyry-epithermal) values are 0 ± 5 ‰, whereas sulfides associated with crustal S sources typically show higher values. The interpretation is

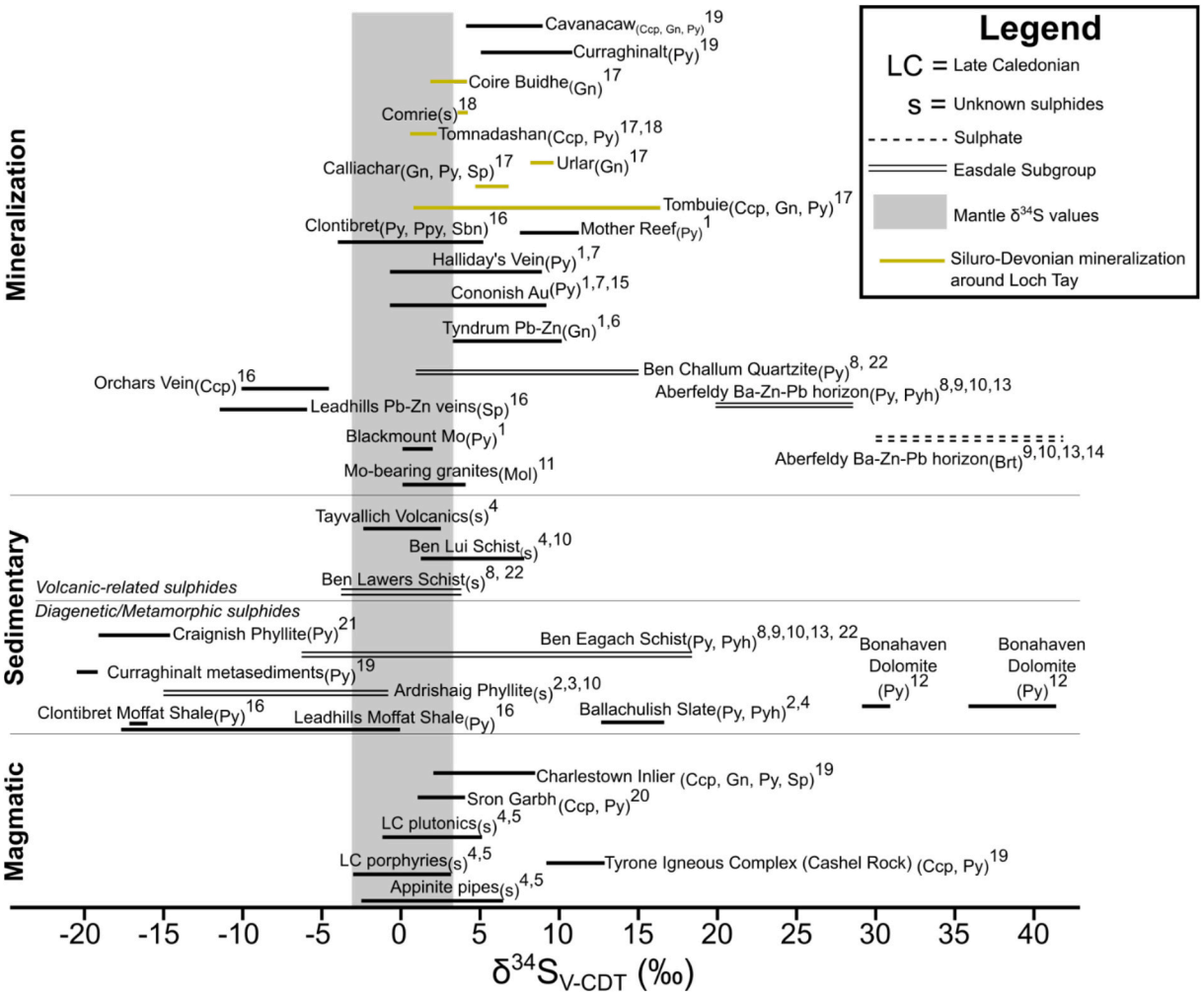

Fig. 6. Compilation of previous $\delta^{34}S$ studies on gold and base metal mineralization throughout Scotland and Ireland, as well as $\delta^{34}S$ values from intrusions and sediments throughout the same region. Mantle-derived melts usually display $\delta^{34}S$ values of 0 ± 3 ‰ (Ohmoto, 1986). The following references were used to compile the data: 1 = Curtis et al. (1993), 2 = Hall et al. (1988), 3 = Hall et al. (1994a), 4 = Lowry (1991), 5 = Lowry et al. (1995), 6 = Pattrick et al. (1983), 7 = Pattrick et al. (1988), 8 = Scott et al. (1987), 9 = Scott et al. (1991), 10 = Willan and Coleman (1983), 11 = Conliffe et al. (2009), 12 = Hall et al. (1994b), 13 = Moles et al. (2014), 14 = Hall et al. (1987), 15 = Spence-Jones et al. (2018), 16 = Rice et al. (2018), 17 = Smith (1996), 18 = Lowry et al. (2005), 19 = Parnell et al. (2000), 20 = Graham et al. (2017), 21 = Parnell et al. (2017), 22 = Hill et al. (2013).

summarized in Fig. 9 and further discussed below (see Fig. 5 for the paragenetic context of the analyzed phases).

Tomnadashan (a known Cu-Mo porphyry) and the Comrie Pluton show clear magmatic affinities with $\delta^{34}S$ values ranging between 0 and +5 ‰ for all of the studied sulfide minerals (Fig. 7). At Coire Buidhe, the galena sulfur data seems to show a bimodal distribution with clusters around 0 ‰ and +5 ‰; the nearby Finglen Vein shows values around +6 ‰. The more depleted signature was derived from in-situ samples whilst the higher signatures were from bulk samples, although only 2–3 data-points in each could be obtained and only galena was analyzed. For Lead Trial, the $\delta^{34}S$ values in galena ranged between −1 and +5 ‰ (n = 13), the in-situ samples again showing a lower profile.

For the rest of the vein systems, the $\delta^{34}S$ values are much higher; Finglen Vein also shows higher signatures for the analyzed sulfides other than galena (Figs. 7, 8). The higher values seem to cluster into two groups: around +6 ‰ for galena and +8 ‰ for other sulfides, and around +8 ‰ for galena (with an outlier at Tombuie of c. 12 ‰) and +11 to +12 ‰ for the other sulfides. Overall, the signatures get higher further away from the magmatic center at Tomnadashan. However, the higher values are seen in samples from the Glen Almond Vein and Tombuie, where the pyrite displays $\delta^{34}S$ values of between +9 to +13 ‰; in-situ samples from the Glen Almond Vein show slightly higher values. The values obtained from galena are significantly lower in the Glen Almond Vein, but not at Tombuie. The Finglen, Calliachar and Urlar veins are generally slightly lower with $\delta^{34}S$ values from pyrite, arsenopyrite and chalcopyrite ranging between +7 and +10 ‰; the galena values are slightly lower for the Finglen Vein and Calliachar, but less so for Urlar. The vein sample V7 (Calliachar Burn; Table 2) shows the most consistent $\delta^{34}S$ values from pyrite (between +8 and +9 ‰). On the other hand, several occurrences of the 'Crustal' veins (Finglen Vein and Urlar Burn) showed examples of some minor intracrystal $\delta^{34}S$ zonation, in which the sulfide rims recorded slightly higher $\delta^{34}S$ values than the core (Fig. 10h, i).

The greater range in the data from pyrite from the isotopically higher 'Crustal' veins (Fig. 8a) may be indicative of a larger amount of heterogeneity associated with this population. However, this trend is not replicated in the galena $\delta^{34}S$ data (Fig. 8b). The galena $\delta^{34}S$ values show a much more homogeneous spread, although the spatial trend for higher signatures away from Tomnadashan is still evident from Fig. 7.

4.2. Pb isotope data

The Pb isotope data derived in this study are depicted in Fig. 11 and in Supplementary Material B (Table B1). The Pb isotope ratios of galena show a clear spatial trend with the ratios being lowest around the

Table 3
Previous fluid inclusion studies on vein quartz from the Loch Tay region. The data was compiled from three sources (Smith, 1996; Ixer et al., 1997; Naden et al., 2010).

Calliachar-Urlar	
Type	**Description**
1	300 °C, 4–8 wt% NaCl; detectable quantities of CH_4C00_3 and N_2
2	$L_{aq} + LCO_2 + VCO_2$, 225–245 °C; 1.4–4.3 wt% NaCl
3	L_{aq} + V, 120–270 °C; 2–13 wt% NaCl
4	L_{aq} + V, 91–175 °C, 10.2–13.7 wt% NaCl, Ca/Mg cations
Tombuie	
Type	**Description**
1	CO_2 abundant, 3.3–15 wt% NaCl
2	Aqueocarbonic inclusions
3	Aqueous, 120–425 °C, 3–14 wt% NaCl
Tomnadashan	
Type	**Description**
1	Aqueocarbonic, >350 °C
2	>300 °C, liquid vapour, host halite and sylvite
3	110–250 °C, 5–10 wt% NaCl
Coire Buidhe	
Type	**Description**
1	Aqueocarbonic, >350 °C
2	Liquid vapour, >300 °C, host halite and sylvite
3	Aqueous, 110–250 °C, 5–10 wt% NaCl
Comrie Pluton	
Type	**Description**
1	35 wt% NaCl, >300 °C

'magmatic' Lead Trial and highest in the 'crustal' Calliachar-Urlar veins (Fig. 11). Samples from the Glen Almond Vein and the Finglen Vein and, to a degree, Coire Buidhe, form intermediate populations between Lead Trial and the veins further to the east. Regarding the individual populations, there is some variation in the ranges between localities. The values from Lead Trial were quite consistent (n = 13) whilst the 'crustal' veins show more variability. The data plot between the Zartman and Doe (1981) lower crust and mantle curves between 400 and 0 Ma (Fig. 11). It is important to note that these curves are global averages and are not region specific. Our results from Loch Tay are also plotted with a range of published Pb isotope data from Ireland and Scotland in Fig. 12.

Calculated model ages for orogenic gold mineralization typically show large degrees of scatter, due to mixing of Pb from multiple sources and/or the contribution of Pb from host rocks during mineralization (Mortensen et al. 2022). Model Pb ages are, however, a useful indicator as to whether different deposits and occurrences may have similar or varied geological histories. Intrusion-related or magmatic-hydrothermal deposits can be expected to have more homogenous compositions than those where additional Pb was derived from external sources. At Loch Tay, model ages vary significantly between localities but are relatively consistent at each site. Ages are oldest for Lead Trial (520–507 Ma), Glen Almond Vein (429 Ma) and Finglen Vein (429–405 Ma), compared to Urlar Burn (419–372 Ma), Coire Buidhe (386–353 Ma), Tomnadashan (379 Ma), Tombuie (365 Ma), and Calliachar (331–317 Ma). Calculated μ ($^{238}U/^{204}Pb$) values cluster at ~ 9.2 to 9.3 for Coire Buidhe, Finglen Vein, Calliachar, Tombuie, and ~ 9.0 for Lead Trial. A single analysis from Tomnadashan yielded a very high μ value of 9.32, whilst samples from the Glen Almond Vein yielded intermediate μ values of ~ 9.1 The interpretation of all the data will be further discussed below.

5. Discussion

Using the paragenetic interpretations (Fig. 5), it is possible to further investigate the isotope data and the fluid events. Gold is associated with chalcopyrite and pyrite at most localities with voluminous galena being later, except for Lead Trial where pyrite is very minor and the voluminous galena stage is coeval with gold mineralization (Fig. 7c). In addition, for Tomnadashan, the $\delta^{34}S$ data from molybdenite is particularly important because these $\delta^{34}S$ values can be linked to the molybdenite Re-Os dates (c. 425–417 Ma; Webb et al., 2024b).

Regarding the sulfur isotope data, the bulk and in-situ values were relatively consistent for the pyrite but for galena, the in-situ values tend to be lower than the bulk data (Fig. 7). There are several explanations for this trend. The bulk analyses may contain contamination from other sulfides, but paragenetic variations may also play a role. For example, at Coire Buidhe, different hand specimens were used in bulk and in-situ analyses, whilst the paragenetic context for the galena is not available at this locality. Therefore, there might be several galena generations here, but a geological control is also possible: Coire Buidhe is the only locality in our study area where the mineralization is hosted in limestone, meaning that dynamic changes in pH during wallrock reactions may have resulted in different $\delta^{34}S$ values. On the other hand, Lead Trial (which is hosted in a felsic metavolcanic sheet) similarly shows significantly lower in-situ galena values compared to the bulk values: here, the gold is paragenetically coeval with the voluminous galena but several galena generations are present (Fig. 5). Unfortunately, no gold was present in the analysed in-situ material so we are unable to judge which $\delta^{34}S$ values relate to the gold mineralization. Regardless, using the in-situ analyses allowed for the targeting of relatively pure portions of the galena crystal (i.e. without inclusions, although inclusions in galena are not common in the Loch Tay area), meaning the in-situ values may be more representative of the $\delta^{34}S$ signature at each of the different localities. The in-situ measurements, on the other hand, target a much smaller region of the crystal, and are therefore perhaps more likely to represent extreme values in the overall range, whilst the bulk measurements may instead reflect a homogenized value for the entire crystal.

The $\delta^{34}S$ dataset from the galena samples typically displays lower values than the measurements derived from the analysis of other sulfides, although this result is expected given the principles of sulfur isotope fractionation. Heavier elements, such as Pb, are able to bond more efficiently with lighter stable isotopes that have higher energy levels (e.g. ^{32}S; Seal, 2006), explaining the relatively depleted $\delta^{34}S$ values derived from the galena samples. It is, therefore, typical for pyrite $\delta^{34}S$ values to be < 2 ‰ higher than values in galena from the same paragenetic generation or fluid flow event (Ohmoto, 1972; Seal, 2006). However, as the discrepancy is often much greater than 2 ‰ and the voluminous galena typically post-dates gold and other sulfides around Loch Tay, the galena data is more likely to reflect a distinct fluid and mineralization event. Even where the pyrite and galena values are near identical (e.g. Tombuie), this does not indicate coeval precipitation of these phases. However, at Tomnadashan the galena (in the Stage 3 quartz veins; Fig. 5) records $\delta^{34}S$ bulk and in situ values that are the same or higher than those measured from Stage 3 pyrite at this locality (Fig. 7), indicating a possible isotopic disequilibrium between pyrite and galena in Stage 3 of the paragenesis of this deposit. Such isotopic disequilibrium can be caused by the dynamic nature of temperature, pH and fO_2 conditions that are associated with porphyry and epithermal mineralization processes (Seal, 2006). At all localities, the influx of meteoric or crustal fluids may have further stimulated changes in the fluid composition (and potentially, the isotopic signature).

5.1. Tomnadashan, Lead Trial and Coire Buidhe

The sulfur isotope profile from the 'Magmatic' mineralization (Fig. 9) is consistent with values commonly reported from I-type granitoids (Ohmoto, 1972; Seal, 2006; Hutchison et al., 2020). The mineralogy and alteration assemblages of Tomnadashan (Webb et al., 2024b; Table 1) are typical of porphyry Cu-Mo mineralization (Simmons et al., 2005; Sillitoe, 2010; Webb, 2024). Re-Os dating of molybdenite at Tomnadashan (c. 425–417 Ma) closely overlaps with the age of several granitoids around Loch Tay (c. 420–418 Ma; Oliver, 2001; Webb et al., 2024b;

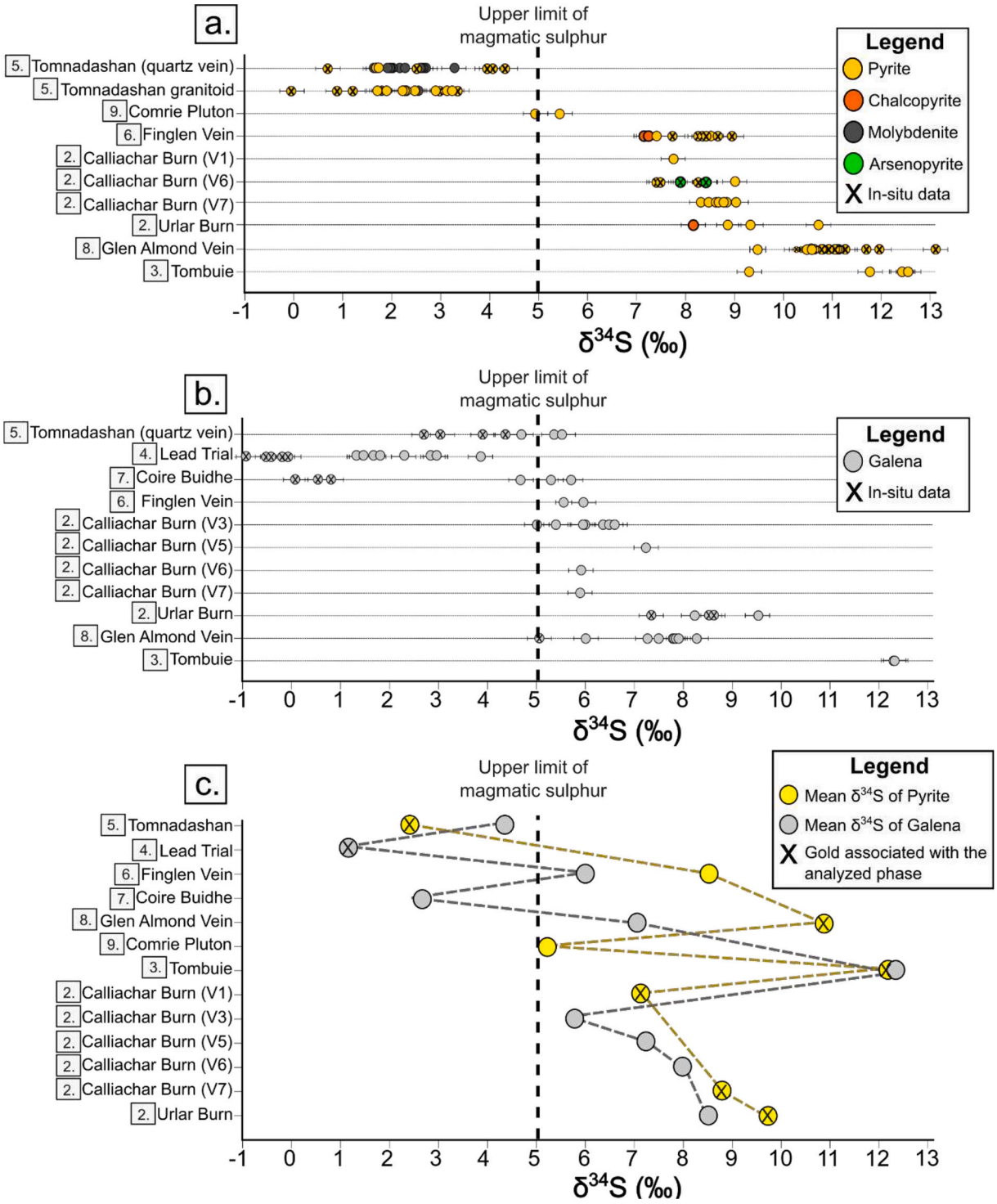

Fig. 7. $\delta^{34}S$ results from this study (the full dataset is presented in Supplementary Material A). a. Pyrite, chalcopyrite, molybdenite and arsenopyrite. b. Galena. c. Mean $\delta^{34}S$ values of pyrite and galena from each locality. It should be noted that with the exception of Lead Trial, voluminous galena paragenetically postdates the other sulfides and gold mineralization (Pattrick, 1984; Ixer et al., 1997; Webb et al., 2024a,b).

Webb, 2024). There is a slight increase in mean $\delta^{34}S$ values from Stage 1 to Stage 3 at Tomnadashan (disseminated sulfides to the quartz veins crosscutting the dissemination). This could be indicative of minor crustal sulfur assimilation and fluid mixing in the later paragenetic stages or, alternatively, a lower temperature of pyrite formation at Stage 3. Therefore, the slight difference in the $\delta^{34}S$ values at Tomnadashan may simply pertain to the nature of porphyry and epithermal environments, where variability may arise from dynamic changes in fO_2, pH and temperature (Börner et al., 2022; McKibben and Eldridge, 1990; Seal, 2006).

In terms of the lead isotopes, the data imply that Pb in the galena was sourced from the mantle and/or lower crust (Fig. 11). This fits well with the geodynamic models of Siluro-Devonian magmatism in Scotland and Ireland suggesting that the granites were derived from melting of the lithospheric mantle and/or the lower crust (Oliver et al., 2008; Miles et al., 2016; Rice et al., 2018). However, slight differences in the μ values

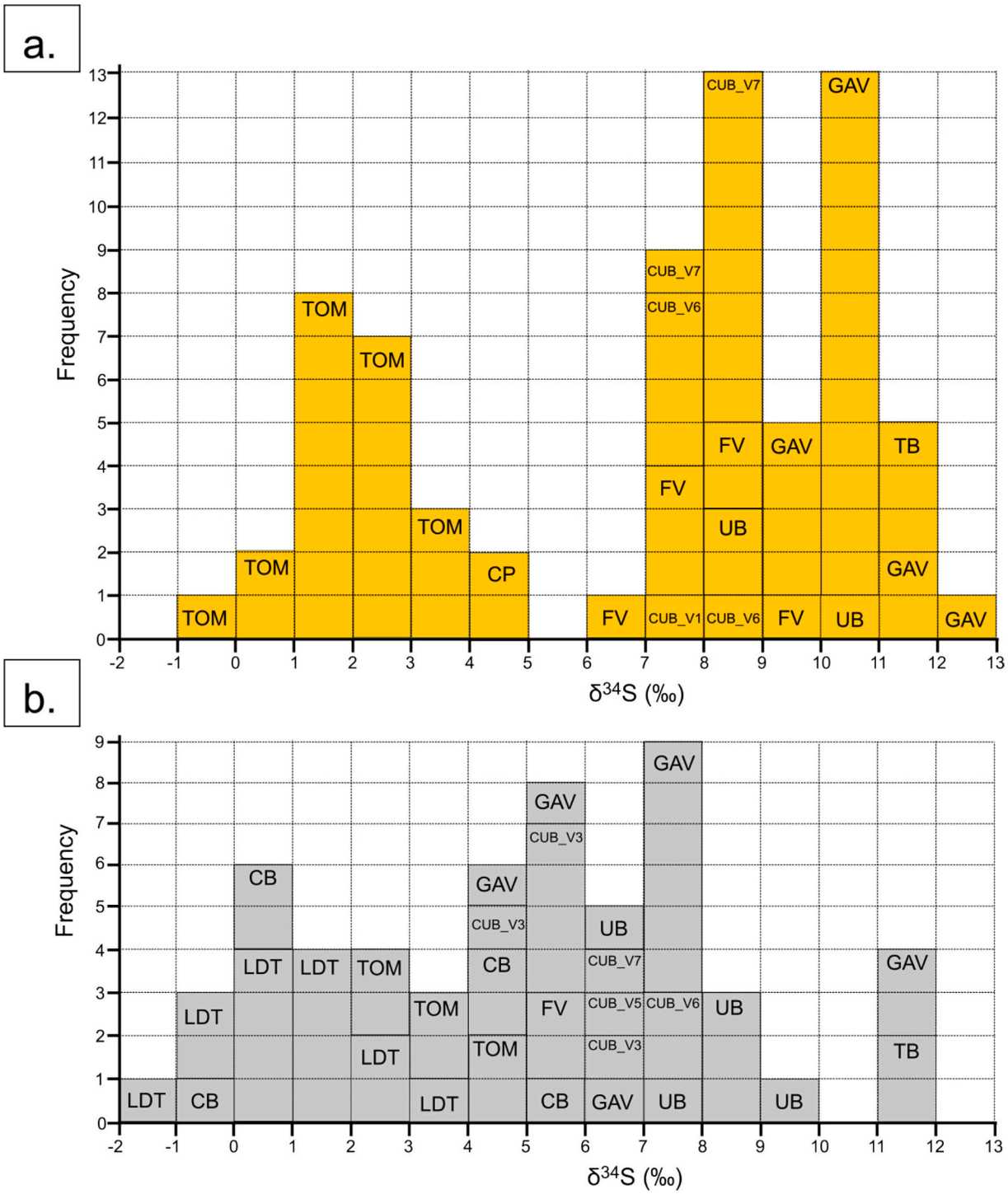

Fig. 8. Frequency of the $\delta^{34}S$ values (measured both in bulk and in-situ; Supplementary Material A, Table A1) in sulfides recorded from the Loch Tay region. a. Pyrite. b. Galena. Abbreviations are as follows: LDT = Lead Trial, TOM = Tomnadashan, CB = Coire Buidhe, CP = Comrie Pluton, FV = Finglen Vein, GAV = Glen Almond Vein, TB = Tombuie, UB = Urlar Burn, CUB = Calliachar Burn (individual veins are given for CUB, e.g., CUB_V3; Fig. 3a).

for Lead Trial and Tomnadashan suggest either subtly different source compositions and/or minor additional crustal incorporation of Pb during fluid flow (Fig. 12). At Lead Trial, galena is paragenetically coeval with other sulfides and gold, whereas at Tomnadashan galena mainly occurs in Stage 3 of the mineralization. Therefore, incorporation of Pb derived from Dalradian metasediments into galena at Tomnadashan may explain the difference in the data. Either way, the evidence is consistent with a magmatic-hydrothermal source for the sulfur, and mantle/lower-crustal lead, at both Lead Trial and Tomnadashan.

5.2. 'Crustal' vein mineralization around Loch Tay

The 'crustal' veins around Loch Tay are hosted in metasediments and show different isotope signatures compared to the 'magmatic' mineralization at Tomnadashan, Lead Trial and Coire Buidhe. The possible reasons for the differences between values obtained from galena and the other sulfides has already been discussed; however, the generally higher $\delta^{34}S$ values of the 'crustal' veins are more typical of crustal sources of sulfur (Ohmoto, 1972; Seal, 2006). It might be tempting to interpret the

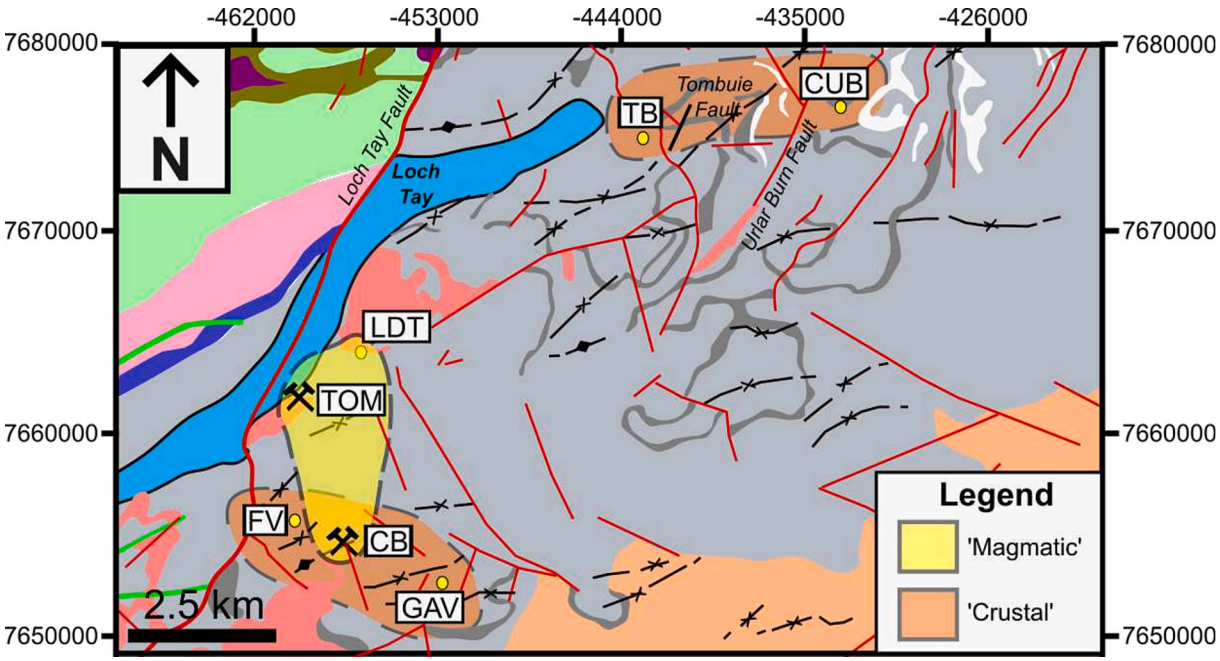

Fig. 9. Distribution of the 'Magmatic' ($\delta^{34}S$ values $<+5$ ‰) and 'Crustal' veins' ($\delta^{34}S$ values $>+5$ ‰) around Loch Tay. The two categories are distinguished on the basis of the upper limit for magmatic sulphur sources (+5 ‰; Hutchison et al. 2020). See Fig. 2 for the legend providing information on the different lithologies. The abbreviations are the same as in Fig. 8.

higher values to arise purely from a non-magmatic fluid (i.e. 'orogenic gold'). However, the Pb isotope profile of the Loch Tay region is considerably less radiogenic than similar datasets from many other occurrences of Phanerozoic gold-bearing mineralization interpreted to represent orogenic gold deposits (Fig. 11; Mortensen et al. 2022). This suggests that the 'crustal' mineralization in the study area is not derived from the upper crust but from the mantle and/or lower crust. It should be noted, however, that some recent models for orogenic gold suggest a significant input from mantle fluids (Groves et al., 2020). Either way, salinities of 13.7 wt% in the Calliachar Burn veins (Ixer et al. 1997) are higher than the values typically associated with orogenic gold mineralization (Ridley and Diamond, 2000; Goldfarb and Groves, 2015) but lower than those typically reported for porphyry deposits (20–60 wt%), although values as low as 5 wt% have been reported further away from the intrusive centres of several porphyries (e.g. in the epithermal parts of the system; Sillitoe, 2000).

Collectively, the available data demonstrates that the 'crustal' veins have characteristics of both magmatic-hydrothermal and crustal fluids. This is difficult to explain with a single fluid source: we suggest that the 'crustal' veins have formed via mixing of fluids originating from both magmatic-hydrothermal and crustal sources. This interpretation is supported by the genetic model of the nearby Cononish Mine (Fig. 1), which suggest that the mineralizing fluids at this locality evolved from an initially magmatic-hydrothermal fluid that progressively mixed with crustal sources over time (Hill et al., 2013; Spence-Jones et al., 2018). The later, higher $\delta^{34}S$ values are also compatible with progressively lower fluid temperatures (Hill et al., 2013). The tendency for the rims of sulfide crystals from the vein-hosted mineralization around Loch Tay to record isotopically higher $\delta^{34}S$ values than the cores may also be indicative of increasing crustal assimilation and/or decreasing temperature. Such $\delta^{34}S$ zonation within individual sulfide crystals is a common feature in magmatic-hydrothermal deposits (McKibben and Eldridge, 1990; Börner et al., 2022). However, it must be stressed that our in-situ dataset is limited (approximately 40 measurements; Supplementary Material A).

Overall, the data are consistent with the interpretation that the mineralizing fluids in the Loch Tay region were initially magmatic-hydrothermal, associated with magmatism derived from the mantle or lower crust; and their isotopic signatures changed over time and spatially in response to various degrees of mixing with crustal sources of sulfur. The differences in Pb isotope ratios between localities (Fig. 11), as well as the variations in model ages and Mu values (Supplementary Material B), can also be explained by incorporation of Pb from various crustal materials, depending on the local host rock. These trends can be observed more widely: the data fit well with the data from Northern Ireland and Ireland (O'Keefe, 1986; Standish et al. 2014; Hollis et al. 2019). In the following section, the nature of the mixing process around Loch Tay is explained in detail, particularly regarding its impact on the isotopic characteristics of the different auriferous veins and the potential lithologies/fluids that were involved.

5.3. *Mixing between magmatic-hydrothermal and crustal fluids around Loch Tay*

Proximally to an intrusion, prograde contact metamorphism may result in crustal fluid release: this process has been indicated for some gold mineralization globally (Fabricio-Silva et al., 2021; Hastie et al., 2021). At Lead Trial and Tomnadashan, the overwhelming majority of $\delta^{34}S$ data clusters within the ranges of magmatic sulfur, suggesting that the impacts of contact metamorphism and fluid mixing at these localities were minor. Rapid ascent of magma, which is typical for porphyry deposits, is also a likely explanation for a low degree of mixing in the Tomnadashan area. Tomnadashan is located adjacent to the Loch Tay Fault (Fig. 2) which at this locality shows a left-stepping kink, consistent with a releasing bend that was likely to facilitate a rapid ascent of the magma. For the Comrie Pluton, whilst a limited amount of $\delta^{34}S$ data is available, the dataset may provide some evidence for a greater degree of crustal assimilation of Dalradian metasediments during the emplacement of the pluton. The $\delta^{34}S$ values of pyrite from the Comrie Pluton (+4.9 and +5.3 ‰) sit outside of the typical range for 'Lower Caledonian' porphyries (−3 to +3 ‰) in the Grampian Terrane (Fig. 6.; Lowry et al. 2005). The relatively high $\delta^{34}S$ values of sulfides from the Comrie Pluton may, therefore, indicate some mixing between magmatic and crustal fluids.

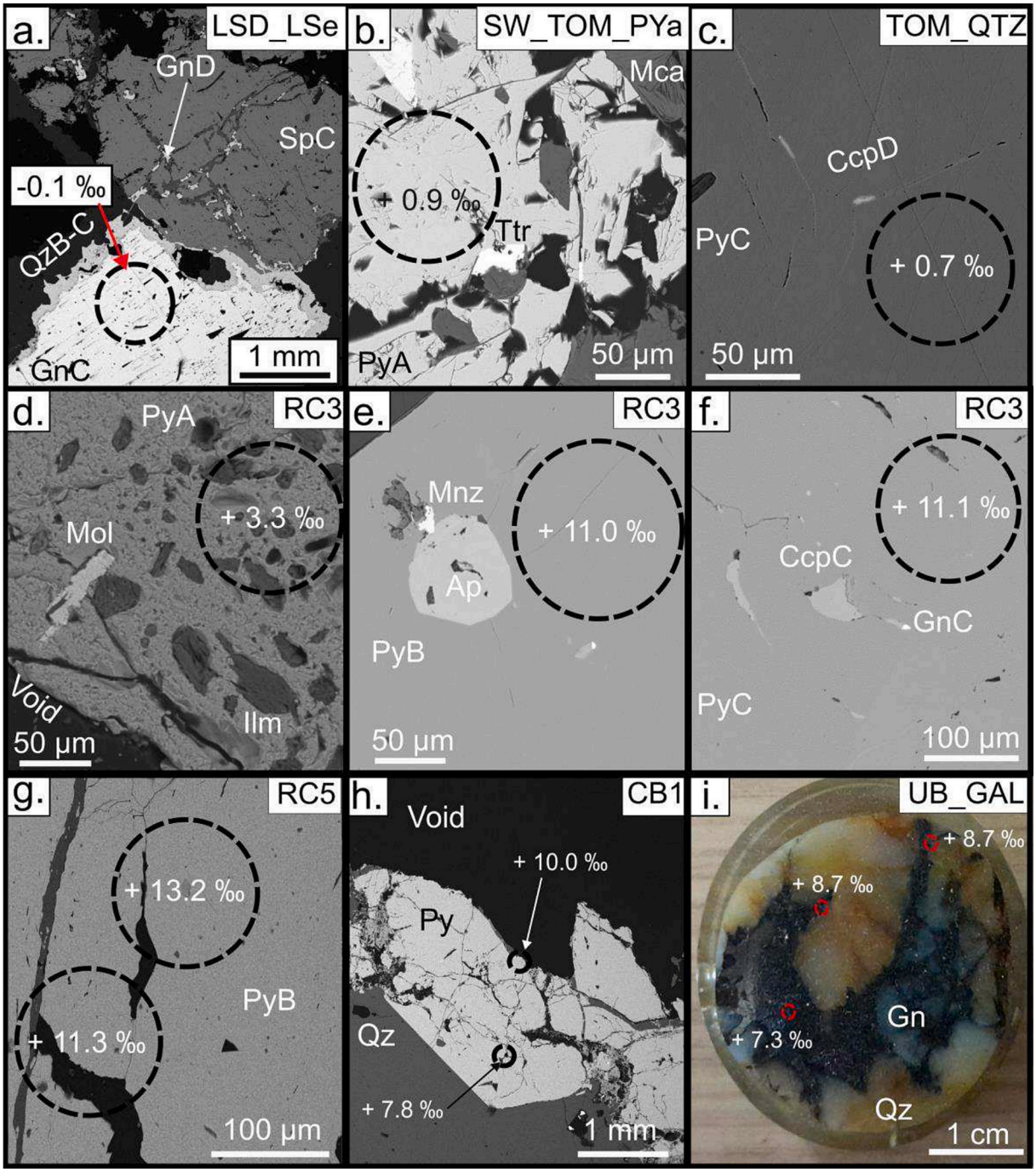

Fig. 10. Petrographic context for selected in-situ $\delta^{34}S$ values (represented by the black/red circles). a. Lead Trial; Stage 3 galena and sphalerite displaying textures typical of mutual intergrowth. This stage of galena precipitation is coeval with gold mineralization (Fig. 5b). b. Tomnadashan; pyrite crystals (PyA) disseminated throughout the host rock overprinted by crosscutting copper sulfosalts belonging to a later paragenetic stage. c. Tomnadashan; Stage 3 PyC, which has been crosscut by CcpD. d. Tomnadashan; disseminated PyA in the granitic host rock. Note the occurrence of molybdenite in the fracture. e. Glen Almond Vein; Stage 2 PyB with inclusions of monazite and apatite (likely the result of coprecipitation). f. Glen Almond Vein; Stage 3 PyC (distinguished based on the As concentration; Webb et al., 2024a). g-i. Several occurrences of $\delta^{34}S$ variations within individual crystals from the Glen Almond Vein (g), Finglen Vein (h) and Urlar Burn (i). The mineral abbreviations of Warr (2021) have been used to indicate the mineral species in each image. (For interpretation of the references to colour in this figure legend, the reader is referred to the web version of this article.)

Distally from Tomnadashan, the magmatic signature becomes increasingly diluted as indicated by the isotopically higher values of the 'crustal' veins. However, given the distance between Tomnadashan and Calliachar-Urlar, we consider it likely that a separate intrusion system exists at depth in the eastern part of the study area. Tombuie is particularly interesting: whilst we obtained isotopically higher $\delta^{34}S$ values (+13 ‰), the data collected by Smith (1996; Fig. 6) show a much wider spectrum of $\delta^{34}S$ values (0 to +16 ‰) from pyrite, chalcopyrite and galena. This is a strong indication of the input of an initially magmatic sulfur source to the veins at Tombuie, although the potential role of remobilization of sulfur from a magmatic host rock (amphibolites) in the vicinity of the veins at Tombuie is unclear (Fig. 3b).

Either way, given the lithological diversity of the study area (Fig. 2), several sources for crustal sulfur are possible. $\delta^{34}S$ values recorded the

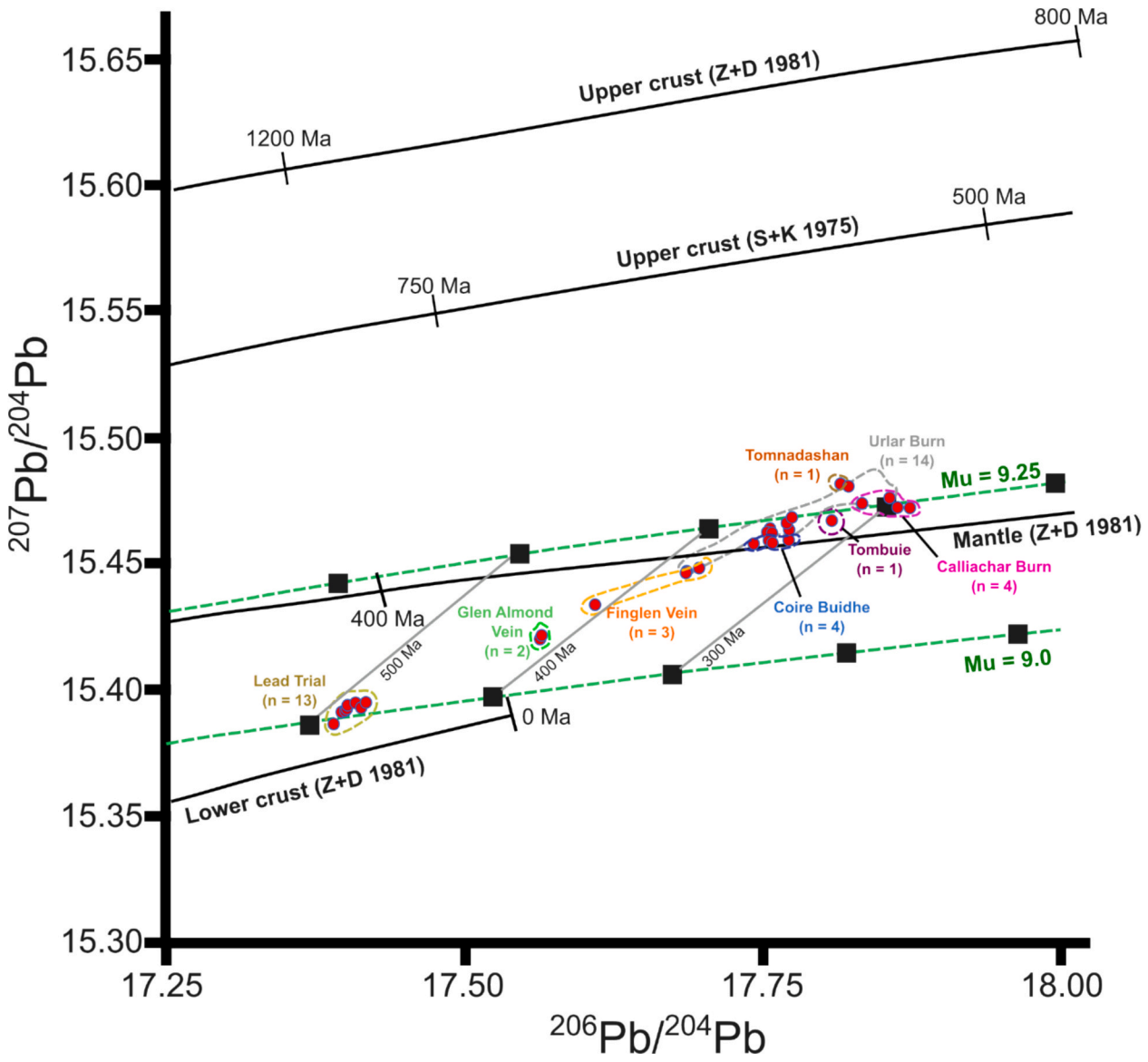

Fig. 11. Pb isotope ratios of galena from different occurrences of mineralization around Loch Tay presented alongside global lead evolution curves produced by Stacey and Kramers (1975) and Zartman and Doe (1981). The full dataset is provided in Supplementary Material B (Table B1).

Dalradian Supergroup metasedimentary and metavolcanic rocks range from −4 to +18 ‰; Fig. 6). Especially interesting are the isotopically very high SEDEX horizons in the Loch Tay area ($\delta^{34}S$ values of 20–25 ‰; Moles et al., 2014): although these are not exposed in our study area, published structural models suggest they are likely to exist at depth due to overturned nappe tectonics (Tanner; 2014a). Mixing between magmatic sulfur and sulfur from Dalradian units (in variable proportions) would be capable of producing sulfides with $\delta^{34}S$ values of between +5 and +12 ‰. Interaction of the magmatic fluids with a variety of lithologies (e.g. shales or ultramafic rocks) could also explain the presence of nickeliferous and Co-bearing phases in some of the veins within the Calliachar Burn, where mafic metavolcanic lithologies are present (Ixer et al., 1997; Chapman et al., 2023). The overlap between the Pb isotope values of the 'crustal' veins around Loch Tay and those reported from SEDEX horizons within the Dalradian Supergroup (including Cononish; Fig. 12) is further evidence in support of an interpretation of mixing with a local crustal source, where Pb was incorporated from SEDEX mineralization (Fig. 2).

Apart from sulfur originating from the Dalradian Supergroup rocks, basinal or meteoric fluids may have played a role in the mixing process. Meteoric fluid influx is known to be an important stimulant of mineralization in several genetic models, including porphyry-epithermal deposits (Hedenquist et al. 1993; Heinrich et al., 2004; Seedorff et al., 2005; Sillitoe, 2015) and orogenic gold mineralization (Pitcairn et al., 2006). Meteoric and basinal fluids can in some cases contain large quantities of sulfur and record isotopically high $\delta^{34}S$ values (> +10 ‰; Seal, 2006). Previous research has advocated for the involvement of meteoric fluids in Scottish gold mineralization, based mostly on fluid inclusion studies (Craw, 1990; Craw and Chamberlain, 1996; Curtis et al., 1993). Furthermore, Ixer et al. (1997) also suggested that the broad range in fluid inclusion temperatures around Loch Tay (e.g. Calliachar-Urlar; Table 3) is compatible with fluid mixing between magmatic or mantle-derived fluids and meteoric fluids.

Collectively, the range of the $\delta^{34}S$ values around Loch Tay of +0.1 to +13.0 ‰ is very similar to what has been observed at Cononish, where a process involving the mixing between magmatic sulfur and sulfur derived from the Dalradian metasediment pile has been invoked (Hill et al. 2013; Spence-Jones et al. 2018). At Cononish, the initial input of magmatic fluids, diluted over time with crustal fluids, was evidenced by the Te fractionation profile reported from this deposit (Spence-Jones

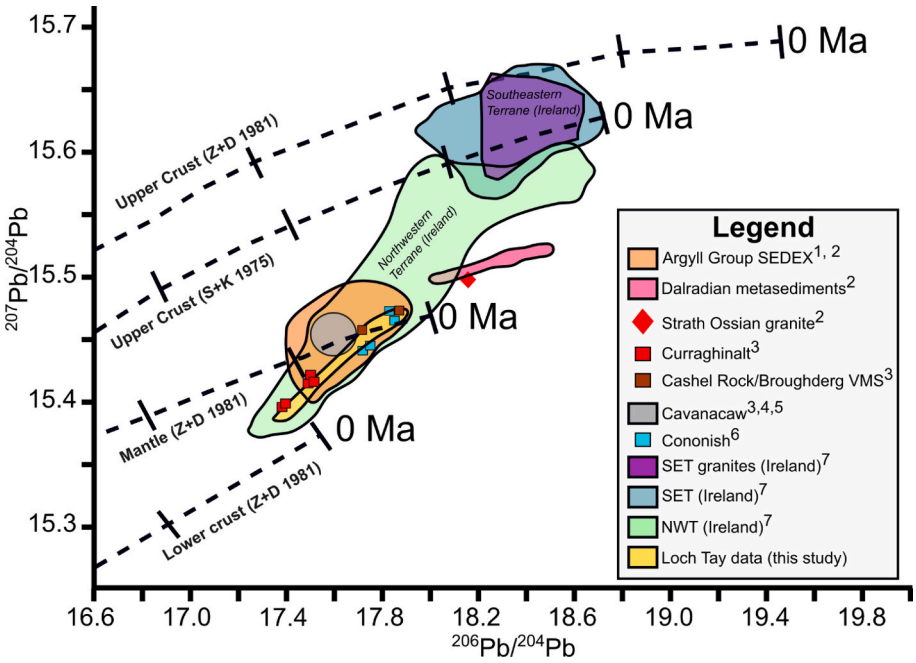

Fig. 12. Pb isotope data from several mineralizations, intrusions and lithologies in the British Isles, including the data from Loch Tay that was collected in this study. SET = Southeastern Terrane, NWT = Northwestern Terrane. All data represents galena, with the exception of the granites (feldspar) and Dalradian metasediments (whole rock data). The dashed lines indicate various Pb evolution models for the Earth (Stacey and Kramers, 1975; Zartman and Doe, 1981), whilst the ticks represent intervals of 400 Ma. 1 = Clayburn et al. (1983), 2 = Clayburn (1988), 3 = Hollis et al. (2019), 4 = Parnell et al. (2000), 5 = O'Keefe (1987), 6 = Swainbank et al. (1981), 7 = Standish et al. (2014).

et al. 2018). Our study did not address Te profiling of the system but the range of $\delta^{34}S$ values is entirely comparable with Cononish. The highest $\delta^{34}S$ values (+13 ‰) from the Loch Tay region (Tombuie and the Glen Almond Vein) are similar to the $\delta^{34}S$ values recorded from Stage 4 Pyrite (late *syn*-Au) at Cononish (+12 ‰; Hill et al., 2013). Hill et al. (2013) calculated that it was not possible for such isotopically high values to develop without a sulfur contribution from the Ben Eagach Schist SEDEX horizons and suggested that the mixing involved two-thirds magmatic and one-third metasedimentary sulfur.

5.4. Model for mineralization

Our findings support the interpretation by Pattrick (1984) of a magmatic (porphyry-epithermal) model for Tomnadashan and Coire

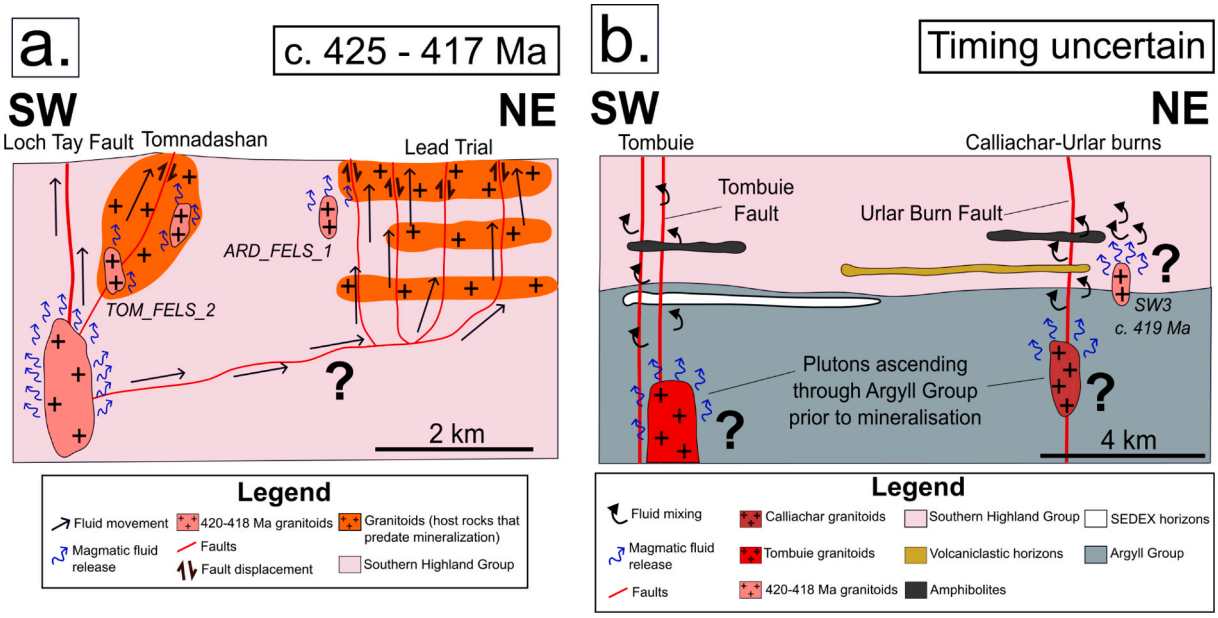

Fig. 13. Genetic model for gold mineralization around Loch Tay. a. Tomnadashan and Lead Trial (c. 425–417 Ma; Webb et al., 2024b); this model also applies to Coire Buidhe where the veins are hosted in limestones. b. Fluid mixing and the development of the 'crustal' veins, using the veins at Tombuie (Fig. 3b) and Calliachar-Urlar (Fig. 3a) as an example. Different lithologies have been added under both localities to illustrate the potential for mineralizing fluids to mix with various lithologies in different parts of the study area. Further investigations are required to constrain the structural characteristics of the Loch Tay region to refine the model and interpret potential fluid flow pathways.

Buidhe; we are able to extend this interpretation to the Lead Trial prospect, which we consider to be a part of the same system (Figs. 9, 13a). The textures and mineralogy of these deposits (Fig. 2) indicate that Tomnadashan comprises a zone of porphyry mineralization, with Lead Trial and Coire Buidhe representing low sulfidation epithermal mineralization. The isotopically higher veins showing evidence of significant fluid mixing (Glen Almond Vein, Finglen Vein, Tombuie, Calliachar-Urlar; Fig. 2) are, with the possible exception of Glen Almond, too far from Tomnadashan to feasibly represent the same magmatic system. Therefore, we discard a model where a magmatic-hydrothermal fluid gradually migrated away from Tomnadashan along structurally controlled conduits, with mixing occurring during a broadly contemporaneous mineralization event on a regional-scale. Our preferred interpretation is that the 'crustal' veins are also epithermal but formed in response to a localized and potentially temporally separate emplacement of igneous intrusion(s) in the eastern parts of the study area (Fig. 13b).

Available geochronology supports our interpretation of a widespread magmatic-hydrothermal mineralising system. Six intrusions in our study area have been dated: the diorite and granitic portions within the Comrie Pluton (425 ± 3 Ma and 404 ± 6 Ma; Oliver et al., 2008), and the four dykes, including one at Calliachar (Fig. 2; c. 420–418 Ma; Webb, 2024). The 420–418 Ma ages of the dykes are practically identical with the c. 425–417 Ma molybdenite Re-Os age for the Tomnadashan mineralization (Webb et al., 2024b). Based on this limited dataset alone, magmatic events around Loch Tay are evident between c. 425–404 Ma. Throughout the wider Loch Tay region, there are several other, undated granitoids that could also have facilitated magmatic-hydrothermal mineralization: for example, small granitoid bodies have been emplaced along the Loch Tay Fault, Urlar Fault and faults at Tombuie (Fig. 3b; Ixer et al., 1997; Treagus, 2000; Corkhill et al., 2010; Naden et al, 2010; Fig. 3a). Furthermore, the association between sulfide mineralization and the c. 404 Ma granite within the Comrie Pluton (Table 1), is evidence for the occurrence of a later mineralization event regionally around Loch Tay. Chapman et al. (2023) suggest that this later event produces a distinct signature in the alluvial gold grains throughout the region. It should also be noted that gold mineralization in the Rhynie Chert and Cononish (Fig. 1) have been dated at 407 ± 1 Ma and 408 ± 1 Ma, respectively (Rice et al., 1995; 2012; Mark et al., 2011). Auriferous mineralization processes related to magmatism are, therefore, known to have occurred throughout the Grampian Terrane in the time interval between c. 420–407 Ma.

The sulfur isotope histograms (Fig. 8) further support the interpretation of separate fluid systems. The pyrite shows a bimodal distribution, with distinct peaks around Tomnadashan (+2 ‰) and the 'crustal' veins (+11 ‰) (Fig. 8a). The lack of any gradation in $\delta^{34}S$ values between the two peaks is consistent with the suggestion that they are associated with distinct fluid systems. The situation is more complex for the paragenetically later galena (Fig. 8b) which shows a wide range of values. This can be explained by increased levels of mixing between magmatic-hydrothermal fluids and local lithologies, resulting in the incorporation of sulfur from a wider range of sources. In addition, in hydrothermal fluids, Pb is typically transported in Cl complexes, as opposed to the bisulfide complex usually associated with gold (Pokrovski et al., 2014). Incorporation of saline basinal fluids in the Early Devonian, when widespread transtension was underway (Dewey and Strachan, 2003), may explain the influx of Cl-rich solutions and remobilization of lead. The broad range in $\delta^{34}S$ values from the galena samples may therefore partially reflect the heterogeneous $\delta^{34}S$ profiles of the Dalradian host rocks. Further evidence for an entirely separate mineralization event is given by the $\delta^{34}S$ data from galena. At Glen Almond, the $\delta^{34}S$ values from galena are, typically, lower than the $\delta^{34}S$ values recorded from pyrite (mean values of +7 and +11 ‰, respectively; Fig. 7c). Galena typically shows lower $\delta^{34}S$ values than a coeval pyrite (Seal, 2006), but the voluminous galena is seen to be paragenetically later than the other phases (Fig. 5). This supports the interpretation that the final mineralization stage involved the influx of an isotopically lower fluid; despite the spread in both the pyrite and galena data, there is no evidence for gradual sulfur fractionation throughout the paragenesis, as would be anticipated from a scenario involving a continuous evolution of the same mineralizing fluid during a single mineralization event.

In summary, the isotopic and paragenetic evidence together strongly point towards an extensive, c. 420–415 Ma magmatic-hydrothermal system responsible for the gold mineralization, followed by a later (Mid-Devonian?), probably basin/extension-related, event remobilizing lead (and zinc) from the Neoproterozoic SEDEX units. However, the studies on gold microchemistry by Chapman et al. (2023; Fig. 4) suggest that a Mid-Devonian magmatic-hydrothermal system may also have operated south of our main study area (at Glen Lednock, Keltie Burn and Sma Glen). This system is probably related to the c. 404 Ma granitic stage of the Comrie Pluton and other, probably coeval intrusions along the Highland Boundary Fault. We did not find evidence that this later magmatic system extends into our main study area, although we cannot exclude the possibility that the late, voluminous galena-sphalerite mineralization included an input from these later magmatic fluids. Either way, this is a mineralization event that we consider to the entirely separate to the gold-bearing event operating around Tomnadashan and in Tombuie-Urlar-Calliachar area.

Future research that could provide further insight into the mineralization processes around Loch Tay may include compositional/trace element mapping of auriferous phases, in order to further refine the understanding of sulfide mineralogy and fluid evolution. Whilst some fluid inclusion data has previously been published (Table 3), there is scope to conduct further fluid inclusion studies to assess regional variations in the temperature of the mineralizing fluids, particularly for some of the newly described localities (e.g. Lead Trial, Glen Almond Vein; Table 2) where no fluid inclusion data exists. Finally, further geochronological constraints on the auriferous veins and intrusions around Loch Tay and the wider Grampian Terrane, combined with high-resolution geophysical datasets, would provide better constraints to the extent of magmatism.

Our findings have wider implications for interpreting vein-hosted gold mineralization. It is clearly possible for magmatic fluids to undergo major changes in their isotopic signature as a result of mixing with crustal fluids, potentially to the extent where the mineralization resembles other deposit styles, particularly orogenic gold. A robust interpretation of deposit models should always involve an appreciation of the wider geological and paragenetic context of the mineralization, whether or not stable isotope or other microanalytical studies are included. In particular, our study illustrates the caveats with relying solely upon stable isotope data to constrain fluid sources: integration of multiple data sources provides a crucial context in which to consider the isotopic datasets.

6. Conclusions

Collectively, the synthesis of our findings with published literature allow us to propose a new, comprehensive model for the Loch Tay mineralization. Our study also demonstrates how some vein-hosted gold deposits that outwardly may resemble 'orogenic gold deposits' are, in fact, related to magmatic-hydrothermal activity (epithermal deposits); this has implications for the interpretation of vein-hosted gold deposits globally. In summary:

1. The mineralizing fluids associated with gold mineralization were derived from granitoid intrusions at c. 425–417 Ma (Fig. 13a). The magmatic signature from sulfur isotopes is well established around Tomnadashan, with the lead isotope data indicating a mantle or lower crustal source for the lead. The magmatic signature becomes increasingly obscure at other vein localities where fluid mixing becomes significant.

2. During mixing, the isotopically higher signature developed as a result of extensive assimilation of sulfur from the Dalradian metasediment package during the emplacement of intrusions in different parts of the region around Loch Tay (Fig. 13b). The Dalradian units include Neoproterozoic SEDEX horizons.
3. A later, Mid-Devonian mineralization event around Loch Tay is expressed as voluminous galena-sphalerite mineralization. It is unclear whether this event is related to the c. 404 Ma magmatic events along the Highland Boundary Fault, or whether it was solely a result of the basin extension processes.
4. Fluid mixing is common in all magmatic-hydrothermal systems globally, and our study demonstrates how this may lead to misinterpretation of vein-hosted gold deposits as 'orogenic'.

The default approach in constraining the fluid sources of vein-hosted deposit studies should, therefore, involve an integrated view where both the paragenetic and wider geological contexts are carefully considered.

Declaration of competing interest

The authors declare that they have no known competing financial interests or personal relationships that could have appeared to influence the work reported in this paper.

Acknowledgements

This research was funded by the Panorama Doctoral Training Partnership and is associated with a grant number (NE/2445151) that is affiliated with the National Environment Research Council. Thanks to Nature Scotland (United Kingdom) for giving permission for sampling to take place at the Tomnadashan Mine in 2022. Furthermore, thanks are extended to National Museums Scotland for providing a sample of mineralization from Tomnadashan (G.2019.101.7), and to the National Museum of Wales for contributing several specimens of mineralization from Tombuie (2003.1G.M.637) and the veins in the Calliachar Burn (2003.1G.M.604 a-p, 2003.1G.M.626 a-v, and 2003.1G.M.630). David Van Acken is thanked for his assistance with Pb isotope analysis at the National Centre for Isotope Geochemistry (NCIG) at University College Dublin (Ireland). Further thanks are extended to various estates around Loch Tay for permitting access and Green Glen Minerals for fieldwork and sampling, as well as Dr Matt Horstwood at the BGS for his assistance with presenting the Pb isotope data.

Appendix A. Supplementary data

Supplementary data to this article can be found online at https://doi.org/10.1016/j.oregeorev.2025.106619.

Data availability

Data will be made available on request.

References

Baron, M., Hillier, S., Rice, C., Czapnik, K., Parnell, J., 2004. Fluids and hydrothermal alteration assemblages in a Devonian gold-bearing hot-spring system, Rhynie, Scotland. Trans. R. Soc. Edinb. Earth Sci. 94 (4), 309–324.

Batchelor, R., 2004a. Air-fall tuffs in the Southern Highland Group, Dalradian Supergroup, at Birnam, Perthshire. Scott. J. Geol. 40 (1), 67–72. https://doi.org/10.1144/sjg40010067.

Batchelor, R., 2004b. More air-fall tuffs from the Southern Highland Group, Dalradian Supergroup, Scotland. Scott. J. Geol. 40 (2), 181–184. https://doi.org/10.1144/sjg40020181.

Baxter, E., Ague, J., Depaolo, D., 2002. Prograde temperature–time evolution in the Barrovian type-locality constrained by Sm/Nd garnet ages from Glen Clova, Scotland. J. Geol. Soc. Lond. 159, 71–82. https://doi.org/10.1144/0016-76901013.

BBC News, 2023. Scotgold: Scotland's only goldmine goes into administration. [Online]. [12th December 2024]. Available from: https://www.bbc.com/news/uk-scotland-tayside-central-67519247.

Börner, F., Keith, M., Bücker, J., Voudouris, P., Klemd, R., Haase, K., Kutzschbach, M., Schiperski, F., 2022. In-situ trace element and S isotope systematics in pyrite from three porphyry-epithermal prospects, Limnos Island, Greece. Front. Earth Sci. 10. https://doi.org/10.3389/feart.2022.916107 article no: 916107 [no pagination].

Bradbury, H. and Smith, R. 1981. Pitlochry. 1:50,000. Keyworth: British Geological Survey.

Chapman, R., Leake, R., Moles, N., 2000. The use of microchemical analysis of alluvial gold grains in mineral exploration: experiences in Britain and Ireland. J. Geochem. Explor. 71 (3), 241–268. https://doi.org/10.1016/S0375-6742(00)00157-6.

Chapman, R., Leake, B., Styles, M., 2002. Microchemical Characterization of Alluvial Gold Grains as an Exploration Tool. Gold Bull. 35 (2), 53–65. https://doi.org/10.1007/BF03214838.

Chapman, R., Torvela, T., Savastano, L., 2023. Insights into regional metallogeny from detailed compositional studies of alluvial gold: an example from the loch Tay Area. Central Scotland. Minerals 13. https://doi.org/10.3390/min13020140.

Chew, D., Strachan, R., 2013. The laurentian caledonides of Scotland and Ireland. Geol. Soc. Lond. Spec. Publ. 390 (1), 45–91. https://doi.org/10.1144/SP390.16.

Clayburn, J., Harmon, R., Pankhurst, R., Brown, J., 1983. Sr, O, and Pb isotope evidence for origin and evolution of Etive Igneous Complex, Scotland. Nature 303, 492–497. https://doi.org/10.1038/303492a0.

Clayburn, J., 1988. The crustal evolution of Central Scotland and the nature of the lower crust: Pb, Nd and Sr isotope evidence from Caledonian granites. Earth Planet. Sci. Lett. 90 (1), 41–51. https://doi.org/10.1016/0012-821X(88)90109-4.

Cooke, D., Simmons, S., 2000. Characteristics and genesis of epithermal gold deposits. Rev. Econ. Geol. 13, 221–244. https://doi.org/10.5382/Rev.13.06.

Cooper, M., Crowley, Q., Hollis, S., Noble, S., Roberts, S., Chew, D., Earls, G., Herrington, R., Merriman, R., 2011. Age constraints and geochemistry of the Ordovician Tyrone Igneous Complex, Northern Ireland: implications for the Grampian orogeny. J. Geol. Soc. London 168 (4), 837–850. https://doi.org/10.1144/0016-76492010-164.

Conliffe, J., Wilton, D., Feely, M., Lynch, E., Selby, D., 2009. S-isotope analyses of molybdenite in the Appalachian–Caledonian Orogen. Abstracts with Programs, Geological Society of America Northeastern section–44th annual meeting. Geological Society of America, Portland (ME). Boulder, CO.

Corkhill, C., Ixer, R., Mason, J., Irving, D., Pattrick, R., 2010. Polymetallic auriferous vein mineralization near Loch Tay, Perthshire. Scotland. Scottish Journal of Geology 46 (1), 23–30. https://doi.org/10.1144/0036-9276/01-378.

Curtis, S., Pattrick, R., Jenkin, G., Fallick, A., Boyce, A., Treagus, J., 1993. Fluid Inclusion and stable isotope study of fault related mineralisation in Tyndrum area, Scotland. Trans. Inst. Mining Metall. (Sect. B: Appl. Earth Sci.) 102, 39–47.

Craw, D., 1990. Regional fluid and metal mobility in the Dalradian metamorphic belt, Southern Grampian Highlands, Scotland. Miner. Deposita 25, 281–288. https://doi.org/10.1007/BF00198998.

Craw, D., Chamberlain, C., 1996. Meteoric incursion and oxygen fronts in the Dalradian metamorphic belt, southwest Scotland: a new hypothesis for regional gold mobility. Miner. Deposita 31 (5), 365–373. https://doi.org/10.1007/BF00189184.

Dallmeyer, R., Strachan, R., Rogers, G., Watt, G., Friend, C., 2001. Dating deformation and cooling in the Caledonian thrust nappes of north Sutherland, Scotland: insights from 40Ar/39Ar and Rb–Sr chronology. J. Geol. Soc. Lond. 158, 501–512. https://doi.org/10.1144/jgs.158.3.501.

Dalradian Resources. 2018. Technical Report for the Curraghinalt Gold Project. Filed on SEDAR. Northern Ireland. Available from: https://minedocs.com/21/CurraghinaltGold-PEA-06222018.pdf.

Damdinov, B., Huang, X., Goryachev, N., Zhmodik, S., Mironov, A., Damdinova, L., Khubanov, V., Reutsky, V., Yudin, D., Travin, A., Posokhov, V., 2021. Intrusion-hosted gold deposits of the southeastern East Sayan (northern Central Asian Orogenic Belt, Russia). Ore Geol. Rev. 139. https://doi.org/10.1016/j.oregeorev.2021.104541 article no: 104541 [no pagination].

Dewey, J., Mange, M., 1999. Petrography of Ordovician and Silurian sediments in the western Irish Caledonides: tracers of a short-lived Ordovician continent – arc collision orogeny and the evolution of the Laurentian Appalachian – Caledonian margin. In: MacNiocaill, C., Ryan, P. (Eds.), Continental Tectonics, 164. Special Publication of the Geological Society, London, pp. 55–107. https://doi.org/10.1144/GSL.SP.1999.164.01.05.

Dewey, J., Strachan, R., 2003. Changing Silurian–Devonian relative plate motion in the Caledonides; sinistral transpression to sinistral transtension. J. Geol. Soc. Lond. 160, 219–229. https://doi.org/10.1144/0016-764902-085.

Dewey, J., 2005. Orogeny can be very short. Proc. Natl. Acad. Sci. 102 (43), 15286–15293. https://doi.org/10.1073/pnas.0505516102.

Digimap.edina.ac.uk. 2023. Digimap. [online] Available at: <https://digimap.edina.ac.uk/os> [Accessed 20 April 2022].

Dirks, P., Sanislav, I., van Ryt, M., Huizenga, J., Blenkinsop, T., Kolling, S., Kwelwa, S., Mwazembe, G., 2020. The world-class gold deposits in the Geita greenstone belt, northwestern Tanzania. In: Sillitoe, R., Goldfarb, R., Robert, F., Simmons, S. (Eds.), Geology of the World's Major Gold Deposits and Provinces. Society of Economic Geologists Special Publication, pp. 163–183. Doi: 10.5382/SP.23.08.

Fabricio-Silva, W., Frimmel, H., Emília Shutesky, M., Rosière, C., Massucatto, A., 2021. Temperature-controlled ore evolution in orogenic gold systems related to synchronous granitic magmatism: An example from the Iron Quadrangle Province, Brazil. Econ. Geol. 116 (4), 937–962. https://doi.org/10.5382/econgeo.4814.

Fielding, I., Johnson, S., Zi, J., Sheppard, S., Rasmussen, B., 2018. Neighbouring orogenic gold deposits may be the products of unrelated mineralizing events. Ore Geol. Rev. 95, 593–603. https://doi.org/10.1016/j.oregeorev.2018.03.011.

Goldfarb, R., Groves, D., Gardoll, S., 2001. Orogenic gold and geologic time: a global synthesis. Ore Geol. Rev. 18 (1–2), 1–75. https://doi.org/10.1016/S0169-1368(01)00016-6.

Goldfarb, R., Baker, T., Dube, B., Groves, D., Hart, C., Gosselin, P., 2005. Distribution, character, and genesis of gold deposits in metamorphic terranes. Econ. Geol. 100, 407–450. https://doi.org/10.5382/AV100.14.
Goldfarb, R., Santosh, M., 2014. The dilemma of the Jiaodong gold deposits: Are they unique? Geosci. Front. 5 (2), 139–153. https://doi.org/10.1016/j.gsf.2013.11.001.
Goldfarb, R., Groves, D., 2015. Orogenic gold: Common or evolving fluid and metal sources through time. Lithos 233, 2–26. https://doi.org/10.1016/j.lithos.2015.07.011.
Goldfarb, R., Pitcairn, I., 2023. Orogenic gold: is a genetic association with magmatism realistic? Miner. Deposita 58 (1), 5–35. https://doi.org/10.1007/s00126-022-01146-8.
Graham, S., Holwell, D., McDonald, I., Jenkin, G., Hill, N., Boyce, A., Smith, J., Sangster, C., 2017. Magmatic Cu-Ni-PGE-Au sulfide mineralisation in alkaline igneous systems: An example from the Sron Garbh intrusion, Tyndrum, Scotland. Ore Geol. Rev. 80, 961–984. https://doi.org/10.1016/j.oregeorev.2016.08.031.
Groves, D., Goldfarb, R., Gebre-Mariam, M., Hagemann, S., Robert, F., 1998. Orogenic gold deposits: a proposed classification in the context of their crustal distribution and relationship to other gold deposit types. Ore Geol. Rev. 13 (1–5), 7–27. https://doi.org/10.1016/S0169-1368(97)00012-7.
Groves, D., Santosh, M., Deng, J., Wang, Q., Yang, L., Zhang, L., 2020. A holistic model for the origin of orogenic gold deposits and its implications for exploration. Miner. Deposita 55 (2), 275–292. https://doi.org/10.1007/s00126-019-00877-5.
Hall, A., Boyce, A., Fallick, A., 1987. Iron sulphides in metasediments: isotopic support for a retrogressive pyrrhotite to pyrite reaction. Chem. Geol. (Isotope Geosci. Sect.) 65, 305–310. https://doi.org/10.1016/0168-9622(87)90010-8.
Hall, A., Boyce, A., Fallick, A., 1988. A sulphur isotope study of iron sulphides in the Late Precambrian Dalradian Easdale Slate Formation, Argyll, Scotland. Mineral. Mag. 52 (367), 483–490. https://doi.org/10.1180/minmag.1988.052.367.06.
Hall, A., Boyce, A., Fallick, A., 1994a. A sulphur isotope study of iron sulphides in the late Precambrian Dalradian Ardrishaig Phyllite Formation, Knapdale, Argyll. Scot. J. Geol. 30 (1), 63–71. https://doi.org/10.1144/sjg30010063.
Hall, A., McConville, P., Boyce, A., Fallick, A., 1994b. Sulphides with high δ34S from the Late Precambrian Bonahaven Dolomite, Argyll, Scotland. Mineral. Mag. 58 (392), 486–490. https://doi.org/10.1180/minmag.1994.058.392.15.
Hastie, E., Schindler, M., Kontak, D., Lafrance, B., 2021. Transport and coarsening of gold nanoparticles in an orogenic deposit by dissolution–reprecipitation and Ostwald ripening. Commun. Earth Environ. 2 (1), 57. https://doi.org/10.1038/s43247-021-00126-6.
He, T., Corso, J., Newton, R., Wignall, P., Mills, B., Todaro, S., Di Stefano, P., Turner, E. C., Jamieson, R.A., Randazzo, V., Rigo, M., Jones, R., Dunhill, A., 2020. An enormous sulphur isotope excursion indicates marine anoxia during the end-Triassic mass extinction. Sci. Adv. 6 (37). https://doi.org/10.1126/sciadv.abb6704.
Hedenquist, J., Simmons, S., Giggenbach, W., Eldridge, C., 1993. White Island, New Zealand, volcanic-hydrothermal system represents the geo-chemical environment of high-sulphidation Cu and Au ore deposition. Geology 21, 731–734. https://doi.org/10.1130/0091-7613(1993)021%3C0731:WINZVH%3E2.3.CO;2.
Heinrich, C., Driesner, T., Stefánsson, A., Seward, T., 2004. Magmatic vapor contraction and the transport of gold from the porphyry environment to epithermal ore deposits. Geology 32 (9), 761–764. https://doi.org/10.1130/G20629.1.
Hill, N., Jenkin, G., Boyce, A., Sangster, C., Catterall, D., Holwell, D., Naden, J., Rice, C., 2013. How the Neoproterozoic S-isotope record illuminates the genesis of vein gold systems: an example from the Dalradian Supergroup in Scotland. Geol. Soc. Lond. Spec. Publ. 393, 213–247. https://doi.org/10.1144/SP393.9.
Hollis, S., Doran, A., Menuge, J., Daly, J., Güven, J., Piercey, S., Cooper, M., Turney, O., Unit, R., 2019. Mapping Pb isotope variations across Ireland: from terrane delineation to deposit-scale fluid flow. In: Proceedings of the 15th SGA Biennial Meeting, 27–30 August 2019, Glasgow, Scotland, pp. 1196–1199.
Hutchison, W., Finch, A., Boyce, A., 2020. The sulphur isotope evolution of magmatic-hydrothermal fluids: insights into ore-forming processes. Geochim. Cosmochim. Acta 288, 176–198. https://doi.org/10.1016/j.gca.2020.07.042.
Ixer, R., Pattrick, R., Stanley, C., 1997. Geology, mineralogy and genesis of gold mineralization at Calliachar-Urlar Burn, Scotland. Trans. Inst. Min. Metall. Sect. B-Appl. Earth Sci. 106, 99–108.
Johnson, C., Breward, N., 2004. G-BASE: geochemical baseline survey of the environment. Keyworth: British Geological Survey. Available from: https://nora.nerc.ac.uk/id/eprint/509527/1/CR04016N.pdf.
Kelley, S., Fallick, A., 1990. High precision spatially resolved analysis of δ34S in sulphides using a laser extraction technique. Geochim. Cosmochim. Acta 54 (3), 883–888. https://doi.org/10.1016/0016-7037(90)90381-T.
Labidi, J., Cartigny, P., Moreira, M., 2013. Non-chondritic sulphur isotope composition of the terrestrial mantle. Nature 501 (7466), 208–211. https://doi.org/10.1038/nature12490.
Lambert-Smith, J., Rocholl, A., Treloar, P., Lawrence, D., 2016. Discriminating fluid source regions in orogenic gold deposits using B-isotopes. Geochim. Cosmochim. Acta 194, 57–76. https://doi.org/10.1016/j.gca.2016.08.025.
Lipson, R., Goldfarb, R., Frieman, B., Payne, J., 2024. San Albino, Nicaragua: A Low-Angle, Thrust-Controlled Orogenic Gold Deposit. Econ. Geol. 119 (2), 395–420. https://doi.org/10.5382/econgeo.5042.
Liu, Y., Zhang, H., Wang, C., 2020. Overprinting by episodic mineralization in the Dongyaozhuang gold deposit, Wutai Mountain, China: Constraints from geology, mineralogy, and fluid inclusions. Geol. J. 55 (8), 5934–5952. https://doi.org/10.1002/gj.3616.
Lowry, D. 1991. The genesis of Late Caledonian granitoid-related mineralisation in Northern Britain. Ph.D. thesis, University of St Andrews. Available from: https://research-repository.st-andrews.ac.uk/handle/10023/3834.
Lowry, D., Boyce, A., Fallick, A., Stephens, W., 1995. Genesis of porphyry and plutonic mineralisation systems in metaluminous granitoids of the Grampian Terrane, Scotland. Trans. R. Soc. Edinb. Earth Sci. 85, 221–237. https://doi.org/10.1017/S0263593300003618.
Lowry, D., Boyce, A., Fallick, A., Stephens, W., Grassineau, N., 2005. Terrane and basement discrimination in northern Britain using sulphur isotopes and mineralogy of ore deposits. Geol. Soc. Lond. Spec. Publ. 248 (1), 264. https://doi.org/10.1144/GSL.SP.2005.248.01.07.
Mark, D., Rice, C., Fallick, A., Trewin, N., Lee, M., Boyce, A., Lee, J., 2011. 40Ar/39Ar dating of hydrothermal activity, biota and gold mineralization in the Rhynie hot-spring system, Aberdeenshire, Scotland. Geochim. Cosmochim. Acta 75 (2), 555–569. https://doi.org/10.1016/j.gca.2010.10.014.
McDivitt, J., Hagemann, S., Thébaud, N., Martin, L., Rankenburg, K., 2021. Deformation, magmatism, and sulfide mineralization in the Archean Golden Mile fault zone, Kalgoorlie gold camp, Western Australia. Econ. Geol. 116 (6), 1285–1308. https://doi.org/10.5382/econgeo.4836.
McKerrow, W., Mac Niocaill, C., Dewey, J., 2000. The Caledonian orogeny redefined. J. Geol. Soc. London 157 (6), 1149–1154. https://doi.org/10.1144/jgs.157.6.1149.
McKibben, M., Eldridge, C., 1990. Radical sulphur isotope zonation of pyrite accompanying boiling and epithermal gold deposition; a SHRIMP study of the Valles Caldera, New Mexico. Econ. Geol. 85 (8), 1917–1925. https://doi.org/10.2113/gsecongeo.85.8.1917.
Mendum, J., Noble, S., 2010. Mid-Devonian sinistral transpression on the Great Glen Fault: the rise of the Rosemarkie Inlier and the Acadian Event in Scotland. In: Law, R., Butler, R., Holdsworth, R., Krabbendam, M., Strachan, R. (Eds.), Continental Tectonics and Mountain Building: the Legacy of Peach and Horne, 335. Special Publication of the Geological Society, London, pp. 161–187. https://doi.org/10.1144/SP335.8.
Menzies, C., Teagle, D., Craw, D., Cox, S., Boyce, A., Barrie, C., Roberts, S., 2014. Incursion of meteoric waters into the ductile regime in an active orogen. Earth Planet. Sci. Lett. 399, 1–13. https://doi.org/10.1016/j.epsl.2014.04.046.
Miles, A., Woodcock, N., Hawkesworth, C., 2016. Tectonic controls on post-subduction granite genesis and emplacement: The late Caledonian suite of Britain and Ireland. Gondw. Res. 39, 250–260. https://doi.org/10.1016/j.gr.2016.02.006.
Moles, N., Boyce, A., Fallick, A., 2014. Abundant sulphate in the Neoproterozoic ocean: implications of constant δ34S of barite in the Aberfeldy SEDEX deposits, Scottish Dalradian. Geol. Soc. Lond. Spec. Publ. 393 (1), 189–212. https://doi.org/10.1144/SP393.7.
Moles, N., Selby, D., 2023. Implications of new geochronological constraints on the Aberfeldy stratiform barite deposits, Scotland, for the depositional continuity and global correlation of the Neoproterozoic Dalradian Supergroup. Precambr. Res. 384. https://doi.org/10.1016/j.precamres.2022.106925 article no: 106925 [no pagination].
Moles, N., Cooper, M., Hollis, S., McConnell, B., 2024. Provenance of the Trainor's Rocks microconglomerate, Northern Ireland: a mid-Silurian (Hawick Group) submarine channel fan deposit in the closing Iapetus Ocean. J. Geol. Soc. London 181 (6), 1–17. https://doi.org/10.1144/jgs2024-025.
Molyneux, S., Harper, D., Cooper, M., Hollis, S., Raine, R., Rushton, A., Smith, M., Stone, P., Williams, M., Woodcock, N., Zalasiewicz, J., 2023. A synopsis of the Ordovician System in its birthplace–Britain and Ireland. Geol. Soc. Lond. Spec. Publ. 532, 191–266. https://doi.org/10.1144/SP532-2022-235.
Mortensen, J., Craw, D., MacKenzie, D., 2022. Concepts and revised models for Phanerozoic orogenic gold deposits. In: Torvela, T., Lambert-Smith, J., Chapman, R. (Eds.), Recent Advances in Understanding Gold Deposits: from Orogeny to Alluvium. Geological Society Special Publications, London. Doi: 10.1144/SP516-2021-39.
Naden, J., Gunn, A., Shephard, T., 2010. Fluids and mineralisation in the Scottish Dalradian. Available from British Geological Survey Internal Report, OR/09/054. https://nora.nerc.ac.uk/id/eprint/531849/1/OR09054.pdf.
Neilson, J., Kokelaar, B., Crowley, Q., 2009. Timing, relations and cause of plutonic and volcanic activity of the Siluro-Devonian post-collision magmatic episode in the Grampian Terrane, Scotland. J. Geol. Soc. Lond. 166, 545–561. https://doi.org/10.1144/0016-76492008-069.
Ohmoto, H., 1972. Systematics of Sulphur and Carbon Isotopes in Hydrothermal Ore Deposits. Econ. Geol. 67 (5), 551–578. https://doi.org/10.2113/gsecongeo.67.5.551.
Ohmoto, H., 1986. Stable isotope geochemistry of ore deposits. Rev. Mineral. Geochem. 16 (1), 491–559. https://doi.org/10.1515/9781501508936-019.
O'Keefe, W., 1986. Age and postulated source rocks for mineralization in Central Ireland, as indicated by lead isotopes. In: Geology and Genesis of Mineral Deposits in Ireland, pp. 617–624.
O'Keefe, W., 1987. A regional lead isotope investigation of mineralization in Ireland. University College Dublin. Ph.D. thesis.
Oliver, G., 2001. Reconstruction of the Grampian episode in Scotland: its place in the Caledonian Orogeny. Tectonophysics 332, 23–49. https://doi.org/10.1016/S0040-1951(00)00248-1.
Oliver, G., Wilde, S., Wan, Y., 2008. Geochronology and geodynamics of Scottish granitoids from the late Neoproterozoic break-up of Rodinia to Palaeozoic collision. J. Geol. Soc. London 165 (3), 661–674. https://doi.org/10.1144/0016-76492007-105.
Parnell, J., Earls, G., Wilkinson, J., Hutton, D., Boyce, A., Fallick, A., Ellam, R., Gleeson, S., Moles, N., Carey, P., Legg, I., 2000. Regional fluid flow and gold mineralization in the Dalradian of the Sperrin Mountains, Northern Ireland. Econ. Geol. 95 (7), 1389–1416. https://doi.org/10.2113/gsecongeo.95.7.1389.
Parnell, J., Perez, M., Armstrong, J., Bullock, L., Feldmann, J., Boyce, A., 2017. A black shale protolith for gold-tellurium mineralisation in the Dalradian Supergroup

(Neoproterozoic) of Britain and Ireland. Appl. Earth Sci. 126 (4), 161–175. https://doi.org/10.1080/03717453.2017.1404682.
Pattrick, R., Coleman, M., Russell, M., 1983. Sulphur isotopic investigation of vein lead-zinc mineralization at Tyndrum, Scotland. Miner. Deposita 18, 477–485. https://doi.org/10.1007/BF00204492.
Pattrick, R., 1984. Sulphide mineralogy of the Tomnadashan copper deposit and the Corrie Buie lead veins, south Loch Tayside, Scotland. Mineral. Mag. 48 (346), 85–91. https://doi.org/10.1180/minmag.1984.048.346.11.
Pattrick, R., Boyce, A., MacIntyre, R., 1988. Gold-Silver vein mineralization at Tyndrum, Scotland. Mineral. Petrol. 38 (1), 61–76. https://doi.org/10.1007/BF01162482.
Phillips, G., Powell, R., 2010. Formation of gold deposits: a metamorphic devolatilization model. J. Metam. Geol. 28 (6), 689–718. https://doi.org/10.1111/j.1525-1314.2010.00887.x.
Pitcairn, I., Teagle, D., Craw, D., Olivo, G., Kerrich, R., Brewer, T.S., 2006. Sources of metals and fluids in orogenic gold deposits: insights from the Otago and Alpine schists, New Zealand. Econ. Geol. 101 (8), 1525–1546. https://doi.org/10.2113/gsecongeo.101.8.1525.
Pitcairn, I., Skelton, A., Wohlgemuth-Ueberwasser, C., 2015. Mobility of gold during metamorphism of the Dalradian in Scotland. Lithos 233, 69–88. https://doi.org/10.1016/j.lithos.2015.05.006.
Pokrovski, G., Akinfiev, N., Borisova, A., Zotov, A., Kouzmanov, K., 2014. Gold speciation and transport in geological fluids: insights from experiments and physical-chemical modelling. In: Garofalo, P., Ridley, J. (Eds.), Gold-Transporting Hydrothermal Fluids in the Earth's Crust. Geological Society of London, London, 10.1144/SP402.4.
Rice, C., Ashcroft, W., Batten, D., Boyce, A., Caulfield, J., Fallick, A., Hole, M., Jones, E., Pearson, M., Rogers, G., Saxton, J., Stuart, F., Trewin, N., Turner, G., 1995. A Devonian auriferous hot spring system, Rhynie, Scotland. J. Geol. Soc. London 152 (2), 229–250. https://doi.org/10.1144/gsjgs.152.2.0229.
Rice, C., Mark, D., Selby, D., Hill, N., 2012. Dating vein-hosted Au deposits in the Caledonides of N. Britain. Trans. Inst. Mining Metall. (Sect B. Appl Earth Sci) 121, 199–200.
Rice, C., Mark, D., Selby, D., Neilson, J., Davidheiser-Kroll, B., 2016. Age and Geologic Setting of Quartz Vein-Hosted Gold Mineralization at Curraghinalt, Northern Ireland: Implications for Genesis and Classification. Econ. Geol. 111 (1), 127–150. https://doi.org/10.2113/econgeo.111.1.127.
Rice, S., Cuthbert, S., Hursthouse, A., 2018. Tectono-magmatic controls of post-subduction gold mineralisation during late Caledonian soft continental collision in the Southern Uplands-Down-Longford Terrane, Britain and Ireland: A review. Ore Geol. Rev. 101, 74–104. https://doi.org/10.1016/j.oregeorev.2018.07.016.
Ridley, J., Diamond, L., 2000. Fluid chemistry of orogenic lode gold deposits and implications for genetic models. In: Hagemann, S., Brown, P. (Eds.), Gold in 2000. Society of Economic Geologists, pp. 141–162. Doi: 10.5382/Rev.13.04.
Scott, R., Pattrick, R., Polya, D., 1987. S isotopic and related studies on Dalradian stratabound mineralisation in the Tyndrum region, Scotland. British Geological Survey, Keyworth.
Scott, R., Pattrick, R., Polya, D., 1991. Origin of sulphur in metamorphosed stratabound mineralisation from the Argyll Group Dalradian of Scotland. Earth Environ. Sci. Trans. R. Soc. Edinb. 82 (2), 91–98. https://doi.org/10.1017/S0263593300007574.
Seal, R., 2006. Sulphur Isotope Geochemistry of Sulfide Minerals. Rev. Mineral. Geochem. 61 (1), 633–677. https://doi.org/10.2138/rmg.2006.61.12.
Searle, M., 2021. Tectonic evolution of the Caledonian orogeny in Scotland: a review based on the timing of magmatism, metamorphism and deformation. Geol. Mag. 159 (1), 124–152. https://doi.org/10.1017/S0016756821000947.
Seedorff, E., Dilles, J., Proffett Jr, J., Einaudi, M., Zurcher, L., Stavast, W., Johnson, D., Barton, M., 2005. Porphyry deposits: Characteristics and origin of hypogene features., 10.5382/AV100.10. In: Economic Geology, 100th Anniversary Volume, pp. 251–298.
Sillitoe, R., Thompson, J., 1998. Intrusion–related vein gold deposits: types, tectono-magmatic settings and difficulties of distinction from orogenic gold deposits. Resour. Geol. 48 (4), 237–250. https://doi.org/10.1111/j.1751-3928.1998.tb00021.x.
Sillitoe, R., 2000. Gold-rich porphyry deposits. In: Hagemann, G., Brown, P. (Eds.), Gold in 2000. Boulder: Society of Economic Geologists, pp. 315–345. Doi: 10.5382/Rev.13.09.
Sillitoe, R., 2010. Porphyry copper systems. Econ. Geol. 105 (1), 3–41. https://doi.org/10.2113/gsecongeo.105.1.3.
Sillitoe, R., 2015. Epithermal paleosurfaces. Miner. Deposita 50 (7), 767–793. https://doi.org/10.1007/s00126-015-0614-z.
Simmons, S., White, N., John, D., 2005. Geological characteristics of epithermal precious and base metal deposits. Econ. Geol. 100, 485–522. https://doi.org/10.5382/AV100.16.
Shaw, J., Torvela, T., Cooper, M., Leslie, G., Chapman, R., 2022. A progressive model for the development of the Cavanacaw Au–Ag–Pb vein deposit, Northern Ireland, and implications for the evolution and metallogeny of the Grampian Terrane. J. Struct. Geol. https://doi.org/10.1016/j.jsg.2022.104637.
Smith, D., 1996. Fractures and mineralisation in the Scottish Dalradian. University of Manchester. Unpublished Ph.D. Thesis.
Smith, C., Gunn, A., Shepherd, T., Coats, J., Wiggans, G., 2003. Gold in the Dalradian Terrane: a review of previous work. BGS Internal Report IR/03/158 191. https://nora.nerc.ac.uk/id/eprint/531850/1/IR03158.pdf.
Smith, C., Livingstone, A., Highton, A., 2022. Chapter 4 Scottish mineral Geological Conservation Review sites – Magmatic and skarn minerals. Proc. Geol. Assoc. 133 (4–5), 350–366. https://doi.org/10.1016/j.pgeola.2019.10.006.
Soper, N., Ryan, P., Dewey, J., 1999. Age of the grampian orogeny in Scotland and Ireland. J. Geol. Soc. Lond. 156, 1231–1236. https://doi.org/10.1144/gsjgs.156.6.1231.
Spence-Jones, C., Jenkin, G., Boyce, A., Hill, N., Sangster, C., 2018. Tellurium, magmatic fluids and orogenic gold: An early magmatic fluid pulse at Cononish Gold Deposit, Scotland. Ore Geol. Rev. 102, 894–905. https://doi.org/10.1016/j.oregeorev.2018.05.014.
Stacey, J., Kramers, J., 1975. Approximation of terrestrial lead isotope evolution by a two-stage model. Earth Planet. Sci. Lett. 26 (2), 207–221. https://doi.org/10.1016/0012-821X(75)90088-6.
Standish, C., Dhuime, B., Chapman, R., Hawkesworth, C., Pike, A., 2014. The genesis of gold mineralisation hosted by orogenic belts: A lead isotope investigation of Irish gold deposits. Chem. Geol. 378–379, 40–51. https://doi.org/10.1016/j.chemgeo.2014.04.012.
Stephenson, D., Mendum, J., Fettes, D., Leslie, A., 2013. The Dalradian rocks of Scotland: an introduction. Proc. Geol. Assoc. 124 (1–2), 3–82. https://doi.org/10.1016/j.pgeola.2012.06.002.
Swainbank, I., Fortey, N., Boast, A., 1981. Lead-Isotope ratios of galena from stratabound mineralization in the Scottish Dalradian. Caledonian-Appalachian Stratabound Sulphides—Symposium Volume. Meeting at University of Strathclyde, Glasgow (20-23).
Tanner, P., 2014a. Structural controls and origin of gold–silver mineralization in the Grampian Terrane of Scotland and Ireland. Geol. Mag. 151 (6), 1072–1094. https://doi.org/10.1017/S0016756813001131.
Tanner, P., 2014b. A kinematic model for the Grampian Orogeny, Scotland. Geol. Soc. Lond. Spec. Publ. 390 (1), 467–511. https://doi.org/10.1144/SP390.23.
Thirlwall, M., 1982. Systematic variation in chemistry and Nd-Sr isotopes across a Caledonian calc-alkaline volcanic arc: implications for source materials. Earth Planet. Sci. Lett. 58 (1), 27–50. https://doi.org/10.1016/0012-821X(82)90101-7.
Thirwall, M., 2002. Multicollector ICP-MS analysis of Pb isotopes, using a (207)Pb-(204) Pb double spike demonstrates up to 400ppm/amu systematic errors in Tl normalization. Chem. Geol. 184 (3–4), 255–279. https://doi.org/10.1016/S0009-2541(01)00365-5.
Thompson, J., Sillitoe, R., Baker, T., Lang, J., Mortensen, J., 1999. Intrusion-related gold deposits associated with tungsten-tin provinces. Miner. Deposita 34, 323–334. https://doi.org/10.1007/s001260050207.
Treagus, J., Pattrick, R., Curtis, S., 1999. Movement and mineralization in the Tyndrum fault zone, Scotland and its regional significance. J. Geol. Soc. Lond. 156, 591–604. https://doi.org/10.1144/gsjgs.156.3.0591.
Treagus, J., 2000. Solid Geology of the Schiehallion District: Memoir for 1: 50000 Geological Sheet 55W (Scotland). Available from Stationery Office. https://webapps.bgs.ac.uk/Memoirs/docs/B06146.html.
Treagus, J., 2003. The Loch Tay Fault: type section geometry and kinematics. Scott. J. Geol. 39 (2), 135–144. https://doi.org/10.1144/sjg39020135.
Warr, L.N., 2021. IMA–CNMNC approved mineral symbols. Mineral. Mag. 85 (3), 291–320. https://doi.org/10.1180/mgm.2021.43.
Webb, S., 2024. Understanding metallogeny around Loch Tay, Scotland: insights from isotope geochemistry and petrographic studies. University of Leeds. Unpublished Ph. D. thesis, Available from: https://etheses.whiterose.ac.uk/35121/.
Webb, S., Torvela, T., Chapman, R., Savastano, L., 2024a. Textural mapping and building a paragenetic interpretation of hydrothermal veins. Geol. Soc. Lond. Spec. Publ. 541 (1). https://doi.org/10.1144/SP541-2023-17.
Webb, S., Torvela, T., Chapman, R., Selby, D., Gooday, R., 2024b. A reinterpretation of the mineralization processes involved in the formation of the Tomnadashan sulfide deposit, Loch Tay, Scotland, UK. Scott. J. Geol. 60 (1). https://doi.org/10.1144/sjg2023-023.
Willan, R., Coleman, M., 1983. S-isotope study of the Aberfeldy barite, zinc, lead deposit and minor sulfide mineralisation in the Dalradian metamorphic terrain, Scotland. Econ. Geol. 78, 1619–1656. https://doi.org/10.2113/gsecongeo.78.8.1619.
Wilson, G., Flett, J., 1921. Special Reports on the Mineral Resources of Great Britain. The Lead, Zinc, Copper And Nickel Ores of Scotland. HMSO, London.
Yardley, B., Cleverley, J., 2013. The role of metamorphic fluids in the formation of ore deposits. Geol. Soc. Lond. Spec. Publ. 393 (1), 117–134. https://doi.org/10.1144/SP393.5.
Zartman, R., Doe, B., 1981. Plumbotectonics—the model. Tectonophysics 75 (1–2), 135–162. https://doi.org/10.1016/0040-1951(81)90213-4.
Zhou, J., 1987. An occurrence of shoshonites near Kilmelford in the Scottish Caledonides and its tectonic implications. J. Geol. Soc. London 144 (5), 699–706. https://doi.org/10.1144/gsjgs.144.5.0699.
Zhou, J., 1988. A gold and silver-bearing subvolcanic centre in the Scottish Caledonides near Lagalochan, Argyllshire. J. Geol. Soc. 145 (2), 225–234. https://doi.org/10.1144/gsjgs.145.2.0225.